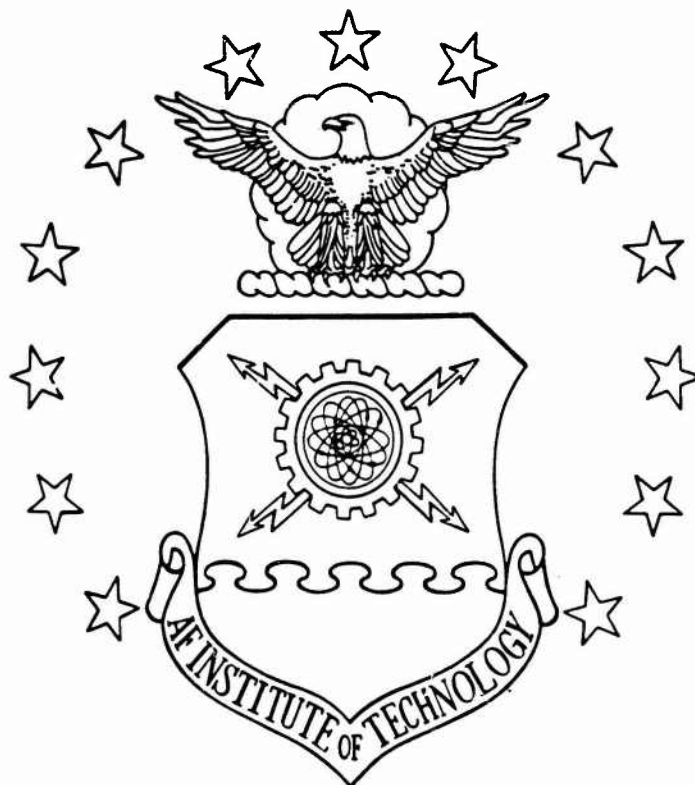AD-A178 851

MULTIPLE ANGLE OF INCIDENCE MEASUREMENT
TECHNIQUE FOR THE PERMITTIVITY AND PERMEABILITY
OF LOSSY MATERIALS AT MILLIMETER WAVELENGTHS

THESIS

John C. Joseph
Second Lieutenant, USAF

AFIT/GE/ENG/86D-58

DTIC
SELECTED
APR 1 3 1987

E

DEPARTMENT OF THE AIR FORCE

AIR UNIVERSITY

AIR FORCE INSTITUTE OF TECHNOLOGY

Wright-Patterson Air Force Base, Ohio

87 4 10 08

- MULTIPLE ANGLE OF INCIDENCE MEASUREMENT
TECHNIQUE FOR THE PERMITTIVITY AND PERMEABILITY
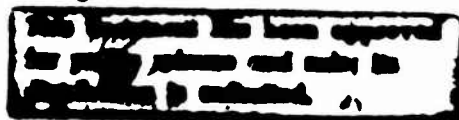OF LOSSY MATERIALS AT MILLIMETER WAVELENGTHS

THESIS

John C. Joseph
Second Lieutenant, USAF

AFIT/GE/ENG/86D-58

DTIC
SELECTE
APR 1 3 1987
S   D
E

AFIT/GE/ENG/86D-58

MULTIPLE ANGLE OF INCIDENCE MEASUREMENT TECHNIQUE

FOR THE PERMITTIVITY AND PERMEABILITY OF LOSSY MATERIALS

AT MILLIMETER WAVELENGTHS

THESIS

Presented to the Faculty of the School of Engineering

of the Air Force Institute of Technology

Air University

In Partial Fulfillment of the

Requirements for the Degree of

Master of Science in Electrical Engineering

John C. Joseph, B.S.

Second Lieutenant, USAF

December 1986

Approved for public release; distribution unlimited

Preface

The purpose of this study was to develop a system to measure the permittivity and permeability of Radar Absorbing Material at millimeter wavelengths. The Avionics Laboratory (AFWAL/AAWP-3) currently has the capability to make material measurements at microwave frequencies, yet modern radar applications may operate well into the millimeter-wave band.

It was intended to test the system at both 56 GHz and 94 GHz. Although the majority of experimentation was performed with the 56 GHz equipment throughout the development of the system, the 56 GHz oscillator failed before completion of the project and no final data was taken at 56 GHz. The absence of data at 56 GHz makes it difficult to draw conclusions about the performance of the system. In addition, failures in the receiver system forced modification of the equipment which ultimately reduced measurement accuracy.

I would like to thank the sponsoring laboratory, in particular Edwin Utt for his contributions to the written product and Dr. Brian Kent who conceived the project. I would like to thank my advisor, Capt R. Jost for his guidance and assistance. Thanks are also due to Dr. Lair and Dr. Jones of the Air Force Institute of Technology for their assistance with the numerical technique and to the Fabrication Shop for the construction of the sample holder assembly. Most of all, I am deeply indebted to my wife Kathy for her help and support. I would also like to acknowledge Kathy and my sons Daniel and Scott for their inspiration, patience, and understanding throughout the course of this project.

<div align="right">John C. Joseph</div>

ii

Table of Contents

List of Figures

List of Tables

Abstract

A technique of measuring the permittivity and permeability of lossy, homogeneous, linear, isotropic materials at millimeter wavelengths was developed. The technique was tested by measurement of representative materials at a frequency of 94 GHz.

For the type of materials under consideration, the permittivity and permeability are complex in general. Thus there are four unknowns to be determined and a minimum of four measurements are required. The approach taken was to measure the magnitude of the transmission coefficient of a planar material sample in free space at multiple angles of incidence. The system of equations obtained from any four of the angles is solved numerically for the permittivity and permeability of the sample.

The equipment consisted primarily of a Gunn phase-locked millimeter-wave oscillator, a pair of conical horn/lens antennae, a sample holder/positioner, and a microwave receiver. Harmonic mixing was employed to convert the test waveform to the operating range of the receiver.

For the case of nonmagnetic materials, best results were obtained if the numerical solution was specialized to incorporate the assumption that the permeability of the material was equal to the permeability of free space. For a material of arbitrary permeability, it was necessary to take data at both perpendicular and parallel polarization of the incident wave to obtain satisfactory results.

MULTIPLE ANGLE OF INCIDENCE MEASUREMENT TECHNIQUE FOR THE PERMITTIVITY
AND PERMEABILITY OF LOSSY MATERIALS AT MILLIMETER WAVELENGTHS

I. Introduction

The effect that a particular material will have on electromagnetic
fields can be predicted if two parameters of the material are known, its
permittivity (ϵ) and its permeability (μ) . There are a number of more
specialized and perhaps more familiar material parameters; such as index
of refraction in optics, intrinsic impedance in microwave engineering,
and power factor in power engineering; but these can all be expressed in
terms of ϵ and μ , which are taken here as the fundamental quantities of
interest. Permittivity and permeability are defined to account for the
effects of a variety of interactions between electromagnetic forces and
the atoms of a material, similar to the manner in which modulus of
elasticity is defined to represent the elastic properties of a material
without consideration of atomic forces in the study of mechanics of
materials.

Permittivity and permeability must be obtained by experimental
methods because calculation of the material parameters is beyond current
theoretical abilities. A technique for measuring ϵ and μ may be based
on any observable interaction between electromagnetic fields and a
material sample. The choice of measurement approach depends on several
considerations. Permittivity and permeability vary with frequency and

1

so must be measured at all frequencies of interest. Although the principles are the same, the nature of test equipment changes drastically with frequency. For example, bridge circuits of inductors and capacitors may be used up to the megahertz range, while interferometers employing mirrors and light sources are used at optical frequencies. Another consideration is the material state (solid, liquid, gas) of the samples to be tested. It is unlikely that a single sample holder will be able to accomodate all potential sample materials, even when restricted to just one material state. It should also be mentioned that a significant trade-off exists between precision and ease/speed of measurement.

The intended application of this measurement facility is the determination of permittivity and permeability of Radar Absorbing Material (RAM). The present state of manufacturing of RAM is such that two samples taken from a single sheet may have a 20 to 50 percent variance in absorber properties (1:68). This large variance has made the goal of extreme precision inappropriate and has created a need for a system to measure sheets of absorber quickly and without special preparation.

Problem and Scope

The aim of this thesis is the design, fabrication, and testing of a system to measure permittivity and permeability at a frequency of 94 GHz by varying the angle of incidence of electromagnetic energy illuminating a sample. Measurement is limited to solid materials in sheet form which are homogeneous, linear, and isotropic. Multi-layered sheets with different materials for each layer are not considered. No further restrictions are made to the permittivity and permeability of the sample material; measurement is not limited to lossless or nonmagnetic materials.

2

Assumptions

In order to determine permittivity and permeability, one must measure the reflection from and/or the transmission through a material sample. For this study, the measurement of transmission is of interest. The derivation of transmission through a sample assumes that an infinite sheet is illuminated by a uniform plane wave. The assumption of a plane wave, which is commonly made in electromagnetic problems, yet physically unrealizable, greatly simplifies the analysis. It is prohibitively difficult to determine the form of the actual field incident on the sample and even more difficult to calculate the transmission of the actual field through the sample. A rigorous development of the actual rather than ideal problem is not warranted because the resulting complexity of measurement and increased computer requirements would defeat the objective of making measurements in a routine fashion, especially in view of the current manufacturing tolerances of RAM. The experimental method of approximating the conditions assumed above will be discussed in Chapter II of this report and the impact the assumptions have on system design will be seen in Chapter IV.

General Approach

The transmission coefficient was calculated for a material of arbitrary ϵ and μ by utilizing a derivation (2:87-92) of plane wave incidence on a dielectric sheet. A numerical technique for determining ϵ and μ from measured values of the transmission coefficient at multiple angles of incidence was devised and implemented. The equipment was assembled and tests were made on materials representative of pure dielectrics, nonmagnetic absorbers, and magnetic absorbers.

3

The information in this thesis is presented in the following order: Chapter II states the objectives and operating conditions of the measurement system. Candidate approaches are discussed and the rationale for the approach selected is given. Chapter III explains the nature of permittivity and permeability and derives the transmission coefficient. The derivation of several supporting relations is given in Appendix A. The design of the equipment set-up and the numerical solution to yield ϵ and μ is given in Chapter IV. Chapter V contains test data and an evaluation of the system. General conclusions and recommendations for further work are given in Chapter VI. Appendix B contains relations needed for the computer codes.

II. Analysis

Material measurement techniques are well established in the direct current to microwave frequency regions and at optical frequencies. These techniques are continually being extended higher and lower in frequency. Due to practical difficulties, the millimeter wave band cannot be handled by either microwave or optical techniques without substantial modification. The system designed for this thesis more closely resembles a microwave than optical system, but features of both approaches are incorporated into this design. This section presents an analysis of the design problem: it outlines several approaches; explains the reasoning for the approach chosen; and shows the influence on the design of the type of materials to be tested, the desired ease of measurement, the desired accuracy, and the test equipment available.

The measurement system is designed to obtain ϵ and μ for homogeneous, linear, isotropic materials. It is intended to measure absorbers so the assumption that the samples are either lossless or nonmagnetic is not made. It will be shown in Chapter III that the permittivity and permeability of such materials are complex in general and hence there are four unknown quantities to be measured: the real and imaginary components of both ϵ and μ.

The emphasis throughout this project has been placed on simplicity of measurement. The degree of precision is limited to the maximum that can be attained with existing equipment and without complicating the measurement process. The test frequency, angle of incidence, and sample thickness are treated as known quantities in the computations. It will

5

be seen that the uncertainty in sample thickness is a large contributor to the total measurement uncertainty. Thickness is measured to a precision of one mil (0.001 inch), but variations in thickness of less than one mil can create significant changes in the transmission coefficient at millimeter-wave frequencies. The wavelength of free space radiation is approximately equal to 126 mils at a frequency of 94 GHz. Therefore, one mil represents approximately 0.008 wavelengths. It is shown in Appendix A that the electrical thickness (thickness in terms of the wavelength within a material) depends on the permittivity and permeability of the material. The wavelength within a material is necessarily smaller than the free space wavelength at the same frequency, thus one mil must represent more than 0.008 wavelengths for any material. A more precise measurement of thickness would not improve results because the thickness of typical samples is not uniform to within one mil. This is especially true for absorbers which have a foam construction.

The system is also constrained by the particular equipment available, a Hughes solid-state continuous wave source of frequency 94 GHz and a Scientific-Atlanta phase-amplitude receiver. An approach is sought that yields a practical experimental procedure as well as an analytically tractable electromagnetic problem. Since an exact solution to plane wave incidence on a plane sheet is available, this approach is followed and an experimental technique that satisfactorily approximates the assumed conditions is investigated. Determination of the four unknown quantities requires four measurements; the potential observables are the amplitude and phase of the reflected and transmitted waves.

Candidate systems for delivering an electromagnetic wave to a

6

material sample can be classified as either guided wave or free space systems. Guided wave systems include hollow waveguide, coaxial line, and various other types of transmission lines, such as microstrip or strip-line. While these methods have had success at microwave frequencies, they are unsuitable in the millimeter wave band. All of the guided wave systems suffer from high transmission loss at millimeter wavelengths. The signal amplitudes are attenuated and measurement sensitivity is reduced, especially for lossy samples. Hollow waveguide and most transmission lines cannot support transverse electromagnetic (TEM) waves, therefore they cannot propagate a plane wave. Coaxial line can support a TEM wave, but at millimeter wavelengths the diameter of the line would have to be very small to avoid propagation of higher order modes. A coaxial sample would require small, precisely machined, toroidal samples. Many materials of interest are simply unsuitable to be prepared in this fashion. Rectangular waveguide would allow for simpler sample shapes, but the small size is still undesirable for measuring RAM because of the inhomogeneities from manufacturing.

The high transmission loss of guided wave systems can be avoided by use of a free space system. The free space wave is a TEM wave, though it has a spherical rather than planar wavefront. The usual method of obtaining a good approximation to plane wave incidence on an object is to place the object a sufficient distance from the antenna. The minimum distance is chosen to set the variation of phase of the incident field across the object to a predetermined amount. To insure a phase variation of no more than $\pi/8$ across an object whose maximum dimension is D, the minimum distance (R) required is given by $R = 2D^2/\lambda$, where λ is

7

the free space wavelength (3:936). Thus R is approximately 12 ft for a 3 in square sample and 48 ft for a 6 in square sample at a frequency of 94 GHz. Since this condition would have to be met for the distance from the sample to the receive antenna as well as the distance from the transmit antenna to the sample, the total distance required would be approximately 25 to 100 ft. In addition to the obvious disadvantage of providing a large space to house such a system are these disadvantages: most of the transmitted energy would not be incident on the sample due to spreading; the total propagation loss for such distances would be high; the signal level available for measurement would be exceedingly low; and it would be necessary to construct an anechoic enclosure to shield against extraneous reflections into the signal path. If the sample is situated close to the antennae, the plane wave assumption is violated but the other problems associated with large distances are eliminated.

The four measurements required may be provided by placing the sample normal to a line joining two antennae directed at each other and measuring both the reflected and transmitted amplitude and phase. This arrangement is rejected because of multiple reflections between the sample and antennae. Also, the reflected wave may be smaller than reflections in the transmit antenna and waveguide components, so the measurement of reflection is unreliable. An alternative to measuring both reflection and transmission is to measure transmission alone under two different conditions; such as varying the frequency, polarization, or angle of incidence of the incident wave or varying the thickness of the sample. Frequency must be ruled out because the source available is

8

not capable of any variation. Also, frequency is unsuitable because the material parameters vary with frequency. Using multiple thicknesses is undesirable because twice the number of samples are required, the assumption that two samples of the same material have identical values of ϵ and μ must be made, and the method relies too heavily on the precision of sample thickness. Polarization is a good possibility if an easy means of changing it can be arranged. It is undesirable if it requires moving the antennae and waveguide. The equipment should be fixed as rigidly as possible since the measurements are sensitive to vibrations. Also, changing the equipment position to vary the polarization increases the time required for measurement.

Varying the angle of incidence is the best choice. The angle is changed by rotating the sample and keeping all other equipment fixed. A large number of sets of data can be taken easily and quickly. The material parameters can be calculated from each set of data and the results averaged to eliminate some of the random measurement error. In addition, the multiple reflections between the sample and antennae are greatly reduced because the other than normal incidence directs the specular reflection away from the antennae.

Since data can be taken at more than four angles of incidence, the four measurements required may be provided by measuring either the amplitude or phase of the transmission coefficient at four angles of incidence. It is decided to measure amplitude alone because amplitude is simpler to measure and simpler to use in the solution for ϵ and μ than is phase.

The measurement approach is to place a planar sample between, but

9

close to, two antennae and measure the amplitude of the wave transmitted through the sample at multiple angles of incidence. The remainder of the system is designed to minimize the error from the assumption of plane wave incidence. An infinite sheet has been assumed in the theoretical calculations so that diffraction effects from the edges of the sample and scattering off the sample holder can be neglected. Experimentally, this condition is approximated by concentrating the incident energy to a small portion of the sample by the use of narrowbeam lens antennae. The lens antennae also serve to improve the planar quality of the incident phase front. It has been shown that the use of a dielectric lens can reduce the minimum range needed for plane wave approximations (4:252-256). The size of the sample and the antenna to sample distance are chosen to yield a desired level of illumination on the edges of the sample according to the particular antenna gain pattern.

The incident wavefront will be spherical rather than purely planar. The effect this has on measurement can qualitatively be compared to the effect of measuring a plane wave incident at a number of slightly different angles of incidence and averaging the results (5:595). The error introduced by the non-planar wavefront can be made negligible by choice of the antenna to sample distances. This is empirically verified by observing the effect of varying these distances on the measured value of a sample of plexiglass. Plexiglass was chosen for the verification rather than a sample of absorber because the material constants of plexiglass are well known.

10

III. Theory

The design of a measurement system depends fundamentally on the nature of the quantities to be measured. Definitions of permittivity and permeability are often given in terms of a particular material application, such as use as a dielectric in a capacitor. The permittivity in this case is derived from the charging current drawn by the capacitor and the loss current in the material. For this reason, it is appropriate to review the theory of permittivity and permeability and to state explicitly what is intended by these terms in this thesis. This section discusses permittivity and permeability for an arbitrary material and then specializes to the case of linear, isotropic materials. The discussion remains general regarding loss and the nature of material loss is described. A derivation of the transmission of a plane wave through a planar sheet is presented next. Subordinate relationships that are needed are derived in Appendix A.

The study of electromagnetics involves four vector field quantities: electric field intensity $\overline{E}$, electric flux density or electric displacement $\overline{D}$, magnetic field intensity $\overline{H}$, and magnetic flux density $\overline{B}$. These four quantities are often reduced to two in practice by means of constitutive relations between the flux density vectors ($\overline{D}$ and $\overline{B}$) and the field intensity vectors ($\overline{E}$ and $\overline{H}$) in a particular medium or material.

Explanations of the constitutive relations are provided in many texts on electromagnetics. A detailed description of the interactions of electromagnetic fields and materials down to the atomic level is

11

given by A. R. von Hippel (6). The information presented here was taken from von Hippel, as well as, Collin (7) and Jones (8).

The constitutive relations express $\overline{D}$ and $\overline{B}$ in terms of $\overline{E}$ and $\overline{H}$ respectively and the material parameters of permittivity and permeability. These parameters are defined to allow one to characterize the effects of materials on fields without consideration of the actual mechanisms acting on individual particles. That is, permittivity and permeability are macroscopic rather than microscopic quantities. The various interactions between particles and fields are summarized by the material properties of polarization, magnetization, and conduction. When an electromagnetic field is applied t᠈ a material, forces are exerted on the particles of the material. The particles are displaced, creating effective electric and magnetic dipoles and possibly a current within the material. Such a current introduces loss since conduction involves the transformation of electrical energy into heat. Polarization ($\overline{P}$) and magnetization ($\overline{M}$) represent the effective electric and magnetic dipole moments per unit volume of the material respectively.

In general ϵ and μ are complex tensor quantities but they reduce to complex scalars for many materials and often can be considered to be real scalars for practical purposes. For instance, in free space the following relations hold:

$$\overline{D}_{fs} = \epsilon_o \overline{E}_{fs} \tag{1}$$

$$\overline{B}_{fs} = \mu_o \overline{H}_{fs} \tag{2}$$

where

12

$$\epsilon_o \approx 1/(36\pi) \quad \times \ 10^{-9} \quad \text{Farads/meter}$$

$$\mu_o = 4\pi \times 10^{-7} \quad \text{Henrys/meter}$$

Free space is a degenerate case of an isotropic medium, a medium whose properties are the same in all directions. The polarization and mag-netization of free space are identically equal to zero. When an electro-magnetic field is applied to an isotropic medium, the resulting polari-zation within the medium is parallel to that of the applied field. If the medium is linear and lossless as well as isotropic, the polarization is directly proportional to the applied field. The effective electric dipole moment represented by P gives rise to a polarization current density $\partial P/\partial t$ which is a source of magnetic field. Maxwell's equation for the curl of $\overline{H}$ states that the source of magnetic field in free space is the displacement current density, $\text{curl}(\overline{H}) = \partial \overline{D}_{fs}/\partial t$. It is con-venient to consider the sum of the free space displacement current densi-ty and the polarization current density as a total displacement current density. This will allow an equation of the form $\overline{D} = \epsilon \overline{E}$ to be written for any lossless, linear, isotropic material, where $\overline{P}$ is accounted for implicitly and

$$\epsilon = \overline{D}/\overline{E} \tag{3}$$

The constitutive relations for lossy, linear, isotropic materials can also be written in the form of Eq (3) if the vectors $\overline{E}$, $\overline{H}$, $\overline{D}$, $\overline{B}$, $\overline{P}$, and $\overline{M}$ are replaced by their corresponding phasors. When losses are present, $\overline{P}$ and $\overline{M}$ are no longer in time phase with $\overline{E}$ and $\overline{H}$. The use of

13

phasors allows one to include the phase difference in the constant of proportionality. Thus for any linear, isotropic material

$$\underline{P} = k_e \underline{E} \qquad (4)$$

$$\underline{M} = k_m \underline{H} \qquad (5)$$

The complex constants of proportionality (k_e and k_m) lead to complex values for ϵ and μ.

Derivation of the Constitutive Relations

Combining the free space displacement and polarization as suggested

$$\underline{D} = \underline{D}_{fs} + \underline{P} \qquad (6)$$

For linear, isotropic materials

$$\underline{D} = \epsilon_o \underline{E} + k_e \underline{E} \qquad (7)$$

$$= (\epsilon_o + k_e) \underline{E} \qquad (8)$$

Permittivity is defined as

$$\epsilon = \underline{D} / \underline{E} \qquad (9)$$

$$= \epsilon_o + k_e \qquad (10)$$

14

The dielectric constant or relative permittivity of a material is defined as

$$\epsilon_r = \epsilon \ / \ \epsilon_o \qquad (11)$$

$$= 1 + k_e \ / \ \epsilon_o \qquad (12)$$

Since k_e cannot be negative, ϵ_r cannot be less than one. Equivalently, ϵ must be greater than or equal to ϵ_o. For lossy materials, ϵ is complex and is written as

$$\epsilon = \epsilon' - j \epsilon'' \qquad (13)$$

$$= \epsilon_o (\epsilon'_r - j \epsilon''_r) \qquad (14)$$

$$\epsilon_r = \epsilon'_r - j \epsilon''_r \qquad (15)$$

where ϵ' and ϵ'' are greater than zero. The minus sign is chosen in Eq (13) because the imaginary part of ϵ must be negative. A positive imaginary part would imply energy creation rather than energy loss.

The development for μ is similar to that for ϵ with one significant difference: the dimensions of $\underline{P}$ and $\underline{D}$ are the same (coulombs/meter^2), while the dimensions of $\underline{M}$ (amperes/meter) are the same as those of $\underline{H}$, not $\underline{B}$. Thus an analog to Eq (6) cannot be written in the form $\underline{B} = \underline{B}_{fs} + \underline{M}$. The objective is to incorporate $\underline{M}$ into an equation of the form $\underline{B} = \mu \underline{H}$. This can be achieved by simply summing $\underline{M}$ and $\underline{H}$.

15

$$\underline{B} = \mu_o \; (\; \underline{H} + \underline{M} \;) \qquad (16)$$

$$= \mu_o \; (\; \underline{H} + k_m \, \underline{H} \;) \qquad (17)$$

$$= \mu_o \; (\; 1 + k_m \;) \, \underline{H} \qquad (18)$$

Permeability is defined as

$$\mu = \underline{B} \; / \; \underline{H} \qquad (19)$$

$$= \mu_o \; (\; 1 + k_m \;) \qquad (20)$$

Relative permeability is defined as

$$\mu_r = \mu \; / \; \mu_o \qquad (21)$$

$$= 1 + k_m \qquad (22)$$

Similar to the electrical constants,

$$k_m \geq 0 \qquad (23)$$

$$\mu_r \geq 1 \qquad (24)$$

$$\mu \geq \mu_o \qquad (25)$$

16

$$\mu = \mu' - j\mu'' \qquad (26)$$

$$\mu_r = \mu'_r - j\mu''_r \qquad (27)$$

Material losses can be attributed to an actual finite conductivity as well as to damping effects associated with the various atomic interactions. Allowing for a conduction current density $\underline{J}$ and a displacement current density $\partial\underline{D}/\partial t$, Maxwell's curl equation for $\underline{H}$ is

$$\text{curl } (\underline{H}) = j\omega \underline{D} + \underline{J} \qquad (28)$$

$$= j\omega\epsilon \underline{E} + \sigma \underline{E} \qquad (29)$$

$$= (j\omega\epsilon + \sigma) \underline{E} \qquad (30)$$

$$= \left[j\omega(\epsilon' - j\epsilon'') + \sigma \right] \underline{E} \qquad (31)$$

$$= (j\omega\epsilon' + \omega\epsilon'' + \sigma) \underline{E} \qquad (32)$$

where

ω = radian frequency

σ = conductivity

and the substitution $\underline{J} = \sigma\underline{E}$ has been made. Since the simple measurement of loss cannot indicate the nature of the actual loss mechanism, it is convenient to represent all the various losses by either an effective conductivity, σ_{eff}, or by an effective imaginary part of the permit-

17

tivity, σ''_{eff}. The first approach yields

$$\text{curl } (\underline{H}) = (j\omega\epsilon' + \sigma_{eff}) \underline{E} \qquad (33)$$

where

$$\sigma_{eff} = \sigma + \omega \epsilon'' \qquad (34)$$

The permittivity is considered to be real (hence lossless); the conduction current density $\underline{J}_{eff} = \sigma_{eff}\underline{E}$ encompasses the entire loss. The second approach yields

$$\text{curl } (\underline{H}) = j\omega (\epsilon' - j \epsilon''_{eff}) \underline{E} \qquad (35)$$

where

$$\epsilon''_{eff} = \epsilon'' + \sigma / \omega \qquad (36)$$

The conduction current density is considered to be zero; the total loss is attributed to a complex ϵ_{eff}, where

$$\epsilon_{eff} = \epsilon' - j \epsilon''_{eff} \qquad (37)$$

Derivation of Transmission Coefficient

The approach taken is to replace the configuration of a plane wave obliquely incident on an infinite sheet in free space with an equivalent transmission line circuit and then use circuit techniques to determine

18

the transmission coefficient (T). The derivation presented here follows material given in (2:79-92).

A cross-sectional view of the problem is shown in Figure 1 where:

d is the thickness of the sample

θ_i is the angle of incidence

$\hat{n}$ is the unit vector outwardly normal to the sample

$\underline{k}$ is the wavenumber vector of the incident wave

The wavenumber is a constant arising from the solution of the time-harmonic wave equation. It is equal to the ratio of (ω) and the velocity of propagation of the electromagnetic wave in the medium (in this case, free space). It can be shown that k is also equal to 2π divided by the wavelength in the medium (2:21).

$$\bar{k} = \hat{x} \, k_x + \hat{y} \, k_y + \hat{z} \, k_z \qquad (38)$$

$$k^2 = |\bar{k}|^2 \qquad (39)$$

$$= k_x^2 + k_y^2 + k_z^2 \qquad (40)$$

$$= \omega^2 \, \mu \, \epsilon \qquad (41)$$

The equivalent circuit is shown in Figure 2, where Z_o and Z_m represent the wave impedance outside and inside the sample sheet respectively. Wave impedance in a given direction is defined as the ratio of the electric and magnetic field components transverse to that direction.

19
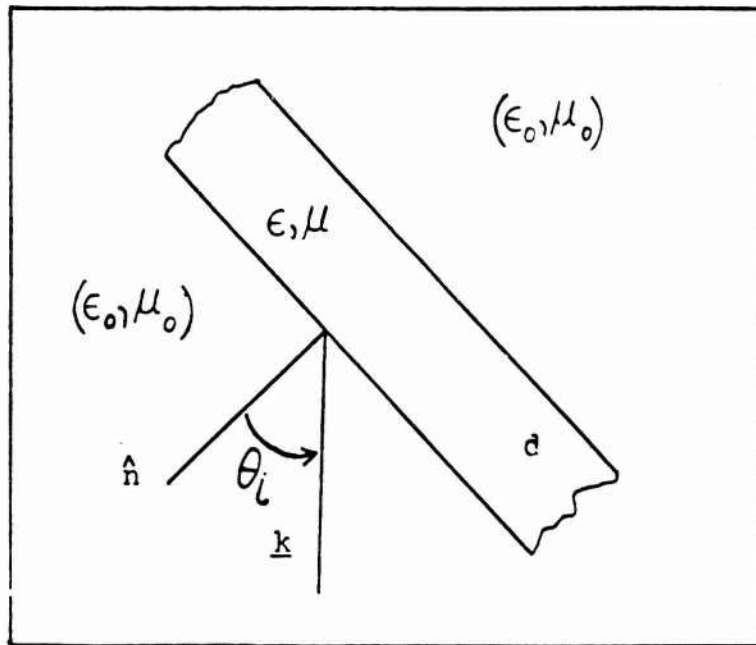
Figure 1.   Geometry for Oblique Incidence
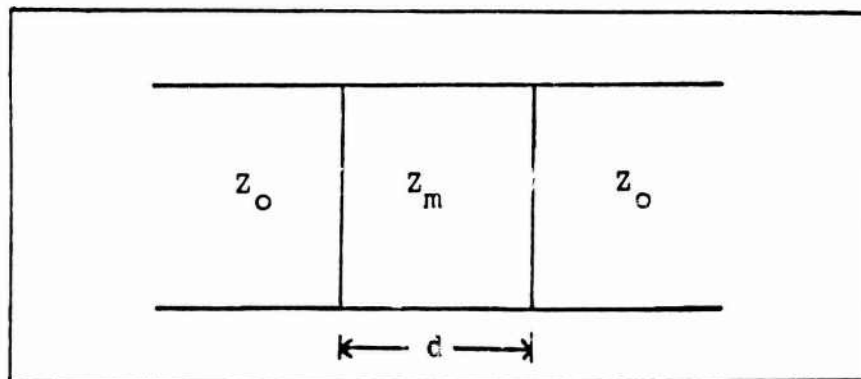
Figure 2.   Equivalent Circuit

The wave impedance is a function of ϵ, μ, θ_i, and the polarization of
the incident wave.

For plane waves, $\underline{E}$ is orthogonal to $\underline{k}$. Two cases of polarization
are considered, parallel and perpendicular. The polarization is paral-
lel when $\underline{E}$ lies in the plane of incidence and perpendicular when $\underline{E}$ is

20
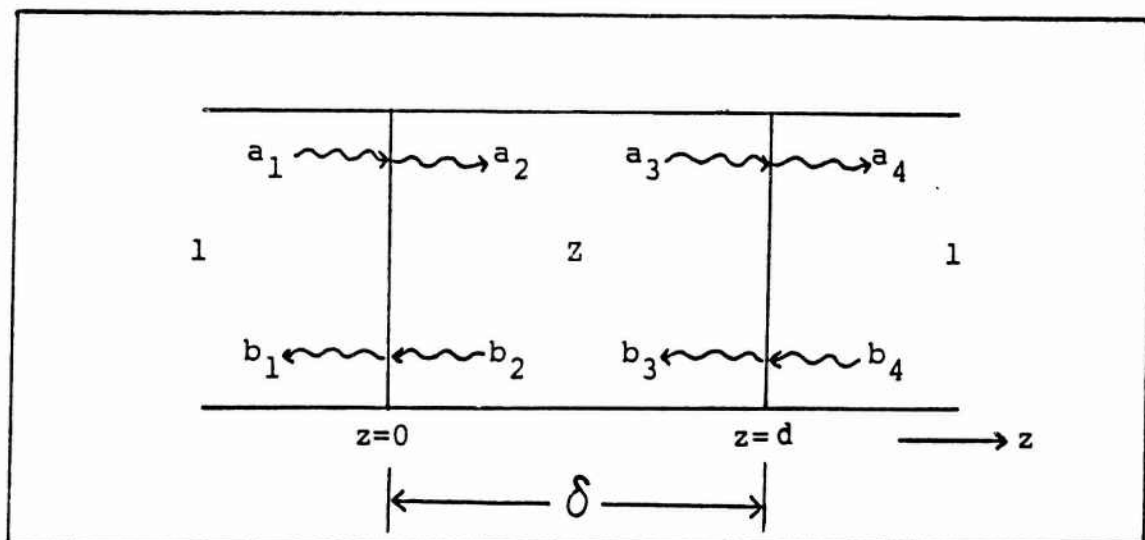
Figure 3. Normalized Equivalent Circuit with Waves Indicated
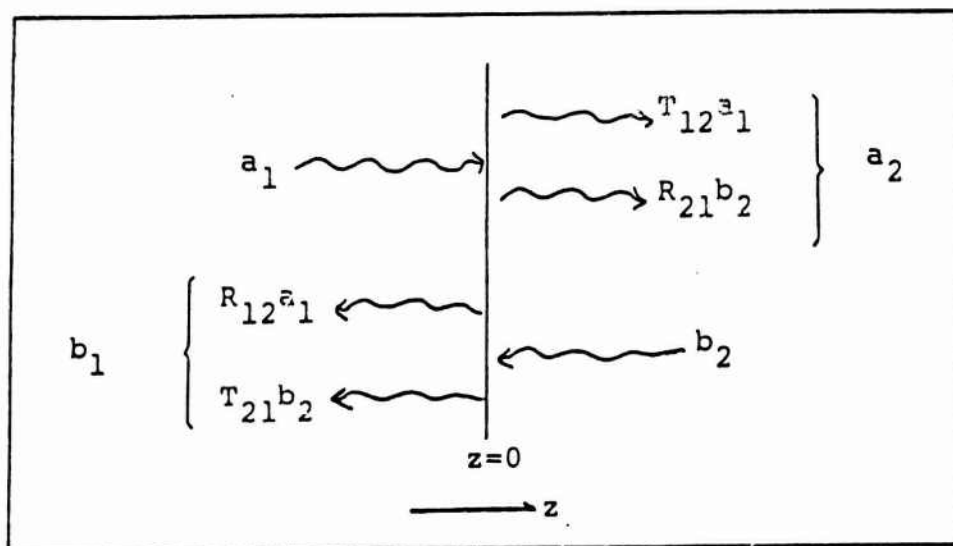
Figure 4. Illustration of Waves at First Boundary

orthogonal to the plane of incidence, where the plane of incidence is the plane containing $\hat{n}$ and $\underline{k}$. It will be seen that T has the same form under either polarization, with the expression for wave impedance corresponding to perpendicular or parallel polarization inserted.

21

The problem at hand is to derive the ratio of transmitted wave (a_4) to incident wave (a_1) for the circuit of Figure 3. The wave impedance has been normalized to that of free space by defining

$$Z = Z_m / Z_o \qquad (42)$$

The electrical thickness of the sample is denoted by σ. The relationship between a_1 and a_4 is due to the effects of the waves traveling through the two boundaries and through the thickness σ. The behavior of the fields at the first boundary is illustrated in Figure 4, where

a_1 is the complex amplitude of the wave indicent from the left

b_2 is the complex amplitude of the wave incident from the right

R_{mn} is the ratio of the amplitudes of the wave reflected from the boundary between regions m and n to the wave incident from region m

T_{mn} is the ratio of amplitudes of the wave transmitted into region n to the wave incident from region m

From Figure 4 and the definitions of R_{mn} and T_{mn}

$$a_2 = T_{12} \, a_1 + R_{21} \, b_2 \qquad (43)$$

$$a_1 = (a_2 - R_{21} \, b_2) \, / \, T_{12} \qquad (44)$$

$$b_1 = R_{12} \, a_1 + T_{21} \, b_2 \qquad (45)$$

$$b_1 = R_{12} \, (a_2 - R_{21} \, b_2) \, / \, T_{12} + T_{21} \, b_2 \qquad (46)$$

22

In matrix form

$$\begin{bmatrix} a_1 \\ b_1 \end{bmatrix} = \frac{1}{T_{12}} \begin{bmatrix} 1 & -R_{21} \\ R_{12} & (T_{12}T_{21} - R_{12}R_{21}) \end{bmatrix} \begin{bmatrix} a_2 \\ b_2 \end{bmatrix} \tag{47}$$

The relationship between a_2 and a_3 is obtained by equating the expressions for the two rightward propagating waves at the right boundary:

$$a_2 \, e^{-j\delta} = a_3 \, e^{0} \tag{48}$$

$$a_2 = a_3 \, e^{j\delta} \tag{49}$$

Similarly

$$b_2 \, e^{j\delta} = b_3 \, e^{0} \tag{50}$$

$$b_2 = b_3 \, e^{-j\delta} \tag{51}$$

In matrix form

$$\begin{bmatrix} a_2 \\ b_2 \end{bmatrix} = \begin{bmatrix} e^{j\delta} & 0 \\ 0 & e^{-j\delta} \end{bmatrix} \begin{bmatrix} a_3 \\ b_3 \end{bmatrix} \tag{52}$$

23

The equation governing the behavior at the second boundary can be written by comparison to the result for the first boundary.

$$\begin{bmatrix} a_3 \\ b_3 \end{bmatrix} = \frac{1}{T_{23}} \begin{bmatrix} 1 & -R_{32} \\ R_{23} & (T_{23}T_{32} - R_{23}R_{32}) \end{bmatrix} \begin{bmatrix} a_4 \\ b_4 \end{bmatrix} \tag{53}$$

Utilizing the definitions of reflection and transmission coefficients in terms of material impedances (2:77)

$$R_{ab} = \frac{Z_b - Z_a}{Z_b + Z_a} \tag{54}$$

and

$$T_{ab} = R_{ab} + 1 \tag{55}$$

yields

$$R_{12} = \frac{Z - 1}{Z + 1} \tag{56}$$

$$R_{21} = \frac{1 - Z}{1 + Z} \tag{57}$$

$$= - R_{12} \tag{58}$$

$$T_{12} = 1 + R_{12} \tag{59}$$

24

$$T_{21} = 1 + R_{21} \tag{60}$$

$$= 1 - R_{12} \tag{61}$$

$$T_{12}T_{21} - R_{12}R_{21} = (1 + R_{12})(1 - R_{12}) - (R_{12})(-R_{12}) \tag{62}$$

$$= 1 - R_{12}^2 + R_{12}^2 \tag{63}$$

$$= 1 \tag{64}$$

Similarly, it can be shown that

$$R_{23} = -R_{32} = -R_{12} \tag{65}$$

$$T_{23} = 1 + R_{23} \tag{66}$$

$$T_{23}T_{32} - R_{23}R_{32} = 1 \tag{67}$$

Eqs (47) and (53) reduce to

$$\begin{bmatrix} a_1 \\ b_1 \end{bmatrix} = \frac{1}{T_{12}} \begin{bmatrix} 1 & R_{12} \\ R_{12} & 1 \end{bmatrix} \begin{bmatrix} a_2 \\ b_2 \end{bmatrix} \tag{68}$$

$$\begin{bmatrix} a_3 \\ b_3 \end{bmatrix} = \frac{1}{T_{23}} \begin{bmatrix} 1 & R_{23} \\ R_{23} & 1 \end{bmatrix} \begin{bmatrix} a_4 \\ b_4 \end{bmatrix} \tag{69}$$

25

To simplify notation, denote R_{12} and $-R_{23}$ by R. Substituting Eqs (52) and (69) into Eq (68) and setting $b_4 = 0$ (since there is not a wave incident from the right)

$$\begin{bmatrix} a_1 \\ b_1 \end{bmatrix} = \frac{1}{T_{12} T_{23}} \begin{bmatrix} 1 & R \\ R & 1 \end{bmatrix} \begin{bmatrix} e^{j\delta} & 0 \\ 0 & e^{-j\delta} \end{bmatrix} \begin{bmatrix} 1 & -R \\ -R & 1 \end{bmatrix} \begin{bmatrix} a_4 \\ 0 \end{bmatrix} \tag{70}$$

Multiplying the matrices and substituting

$$T_{12} T_{23} = (1 + R)(1 - R) \tag{71}$$

$$= 1 - R^2 \tag{72}$$

yields

$$\begin{bmatrix} a_1 \\ b_1 \end{bmatrix} = \frac{1}{1-R^2} \begin{bmatrix} e^{j\delta} - R^2 e^{-j\delta} & R(e^{-j\delta} - e^{j\delta}) \\ R(e^{j\delta} - e^{-j\delta}) & e^{-j\delta} - R^2 e^{j\delta} \end{bmatrix} \begin{bmatrix} a_4 \\ 0 \end{bmatrix} \tag{73}$$

The overall transmission coefficient T is equal to a_4/a_1.

$$a_1 = \frac{e^{j\delta} - R^2 e^{-j\delta}}{1 - R^2} a_4 \tag{74}$$

$$T = \frac{1 - R^2}{e^{j\delta} - R^2 e^{-j\delta}} \tag{75}$$

26

$$= \frac{1 - (\frac{Z-1}{Z+1})^2}{e^{j\delta} - (\frac{Z-1}{Z+1})^2 e^{-j\delta}} \qquad (76)$$

$$= \frac{(Z+1)^2 - (Z-1)^2}{(Z+1)^2 e^{j\delta} - (Z-1)^2 e^{-j\delta}} \qquad (77)$$

$$T = \frac{4\,Z}{(Z+1)^2 e^{j\delta} - (Z-1)^2 e^{-j\delta}} \qquad (78)$$

The denominator can be simplified to

$$\text{denominator} = (Z^2+2Z+1)e^{j\delta} - (Z^2-2Z+1)e^{-j\delta} \qquad (79)$$

$$= (Z^2+1)(e^{j\delta}-e^{-j\delta}) + 2Z(e^{j\delta}+e^{-j\delta}) \qquad (80)$$

$$= (Z^2+1)[2j\,\sin(\delta)] + 2Z[2\,\cos(\delta)] \qquad (81)$$

$$= 4Z\,\cos(\delta) + 2j(Z^2+1)\,\sin(\delta) \qquad (82)$$

From Eqs (78) and (82)

$$T = \frac{4\,Z}{4\,Z\,\cos(\delta) + 2j(Z^2+1)\,\sin(\delta)} \qquad (83)$$

$$= \frac{1}{\cos(\delta) + \frac{2j(Z^2+1)}{4\,Z}\,\sin(\delta)} \qquad (34)$$

27

$$= \frac{1}{\cos(\delta) + \frac{j}{2} (Z+\frac{1}{Z}) \sin(\delta)} \qquad (85)$$

so

$$T = \left[\cos(\delta) + (\frac{j}{2})(Z+\frac{1}{Z}) \sin(\delta)\right]^{-1} \qquad (86)$$

For perpendicular polarization

$$Z = \frac{\mu_r \cos(\theta_i)}{[\mu_r \epsilon_r - \sin^2(\theta_i)]^{\frac{1}{2}}} \qquad (87)$$

For parallel polarization

$$Z = \frac{[\mu_r \epsilon_r - \sin^2(\theta_i)]^{\frac{1}{2}}}{\epsilon_r \cos(\theta_i)} \qquad (88)$$

The electrical thickness of the sheet is the same for both

$$\delta = 2\pi(\frac{d}{\lambda_o}) [\mu_r \epsilon_r - \sin^2(\theta_i)]^{\frac{1}{2}} \qquad (89)$$

The derivations of Z and δ appear in Appendix A.

By utilizing Eqs (86), (87), (88), and (89), it is possible to determine ϵ_r and μ_r from measurement of T. The method of solving these equations is shown in Chapter IV.

IV. Design

The basic approach taken to the design of the measurement system was presented in Chapter II. Due to the limited power available from the millimeter wave source and the relatively high insertion loss associated with millimeter waveguide components, an approach was pursued that led to minimum usage of millimeter wave equipment. Measurement of absorber is restricted by the sensitivity of the receiver and the power level at the input to the receiver. To achieve the maximum dynamic range possible, the waveguide loss must be minimized and the test frequency must be converted to the operating range of the receiver as efficiently as possible. It will be seen that the simplicity of measurement results in complexity of the computer inversion of the measured data to yield ϵ and μ. This section provides the details of the design and points out the influence of several practical considerations on the design. The equipment set-up is discussed first followed by the computer implementation of the numerical solution.

Equipment Design

A simplified block diagram of the test equipment appears in Figure 5.a. The primary components are the millimeter wave oscillator, the receiver subsystem, and the antenna/sample holder assembly. A photograph of the antenna and sample holder is given in Figure 5.b. The assembly provides a rigid support for the antennae and the sample and allows accurate positioning of the sample. The assembly is constructed almost entirely of wood to minimize unwanted reflections. Plastic bolts are used to secure the sample to the wooden frame. The antenna supports

29
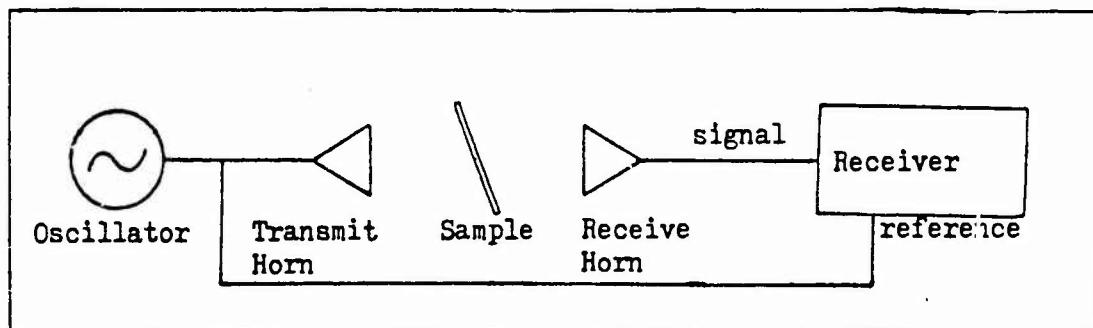
Figure 5.a   Simplified Block Diagram
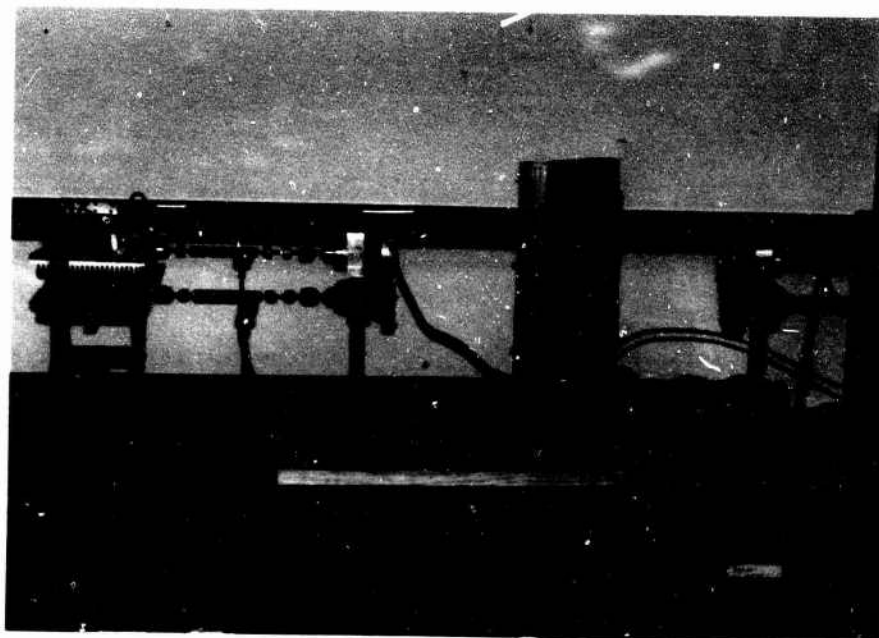
Figure 5.b   Antenna/Sample Holder Assembly

are metal because maximum stability of the antennae is needed and reflec-
tions from the antenna supports are not noticeable.

Ideally, it is desired to transmit a plane wave onto a material
sample without illuminating external objects or the sample holder.
Since this cannot be achieved in practice, a compromise must be made
that involves: the antenna characteristics, the level of illumination
of the sample holder, and the choice of sample size (A), maximum angle

30

of incidence (θ_{max}), and antenna to sample distance (R).

The necessity of confining virtually all of the energy radiated by the transmit antenna to a portion of the sample requires the use of a narrow beamwidth antenna. The antenna's amplitude pattern is therefore strongly non-planar, yet a nearly planar phase pattern can still be achieved by fitting the antenna aperture with a properly shaped dielectric lens. The effect of the lens is to convert the phase front from spherical to planar as illustrated schematically in Figure 6. The transmit and receive antennae are the same model: a conical horn with a plano-convex lens. The amplitude pattern of the antenna is given in Figure 7.

The following considerations should be kept in mind during the derivation of the relation between R, A, θ_{max}, and the antenna beamwidth γ:

1. the larger R is, the more planar is the incident wave across the sample

2. the choice of γ depends on the maximum allowable illumination level of the sample holder

3. the greater A is the wider the range of incidence angles that can be used. It will be seen that more varied values of θ_i are desirable for the numerical solution.

4. There is a practical limit to the sample size A.

As θ_i is increased from normal incidence $(\theta_i = 0°)$, the antenna beamwidths subtend a larger area on the surface of the sample. This effect is more pronounced in the horizontal plane than the vertical, since the sample is rotated about a vertical line. The antenna beamwidth, E-plane

31
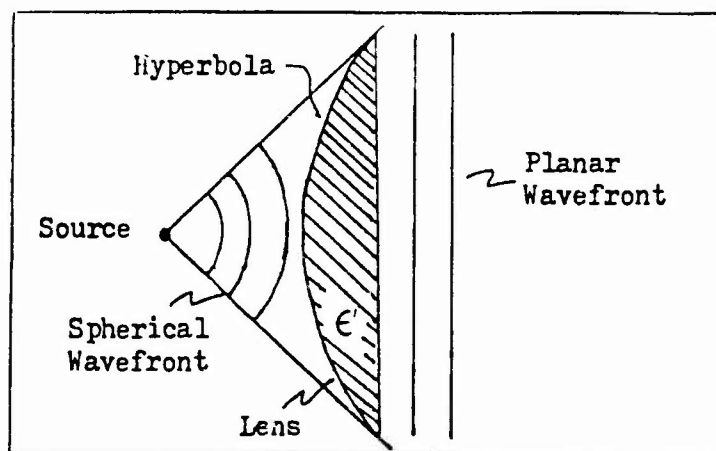
Figure 6. Transformation of Spherical to Planar Wavefront (9:691)
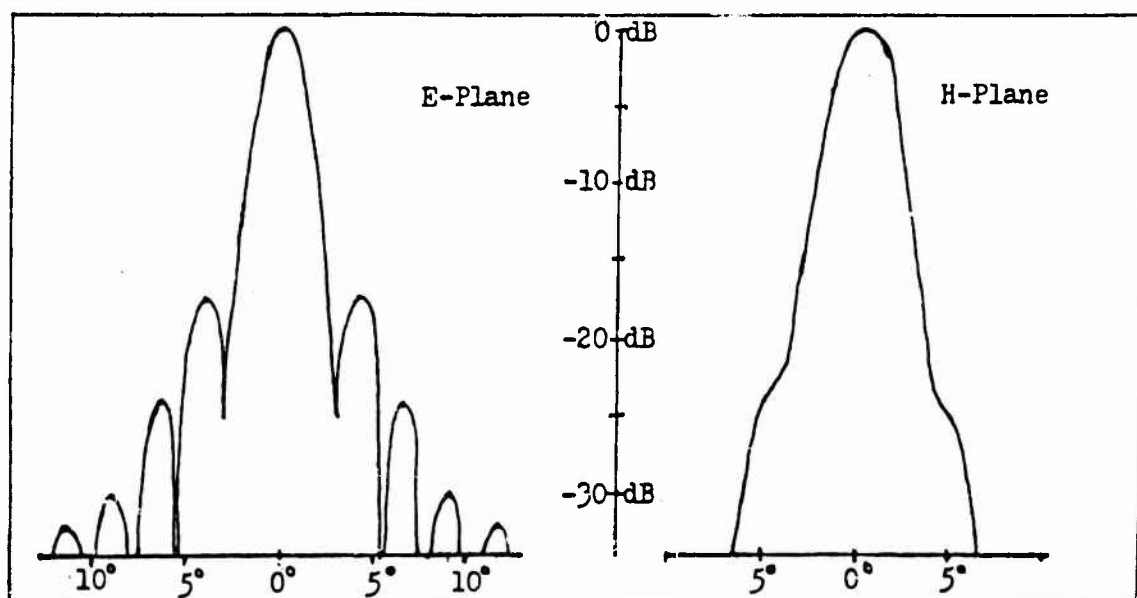
Figure 7. Antenna Amplitude Pattern

or H-plane, that lies in the horizontal plane depends on the polariza-
tion of the incident wave: for perpendicular polarization the H field
is in the horizontal plane and the H-plane beamwidth is used in calcula-
tions involving γ; for parallel polarization the E-plane beamwidth is
substituted for γ. The width (w) of the sample must be large enough to
encompass the entire projection of γ on the sample for $\theta_1 = \theta_{max}$. If

32
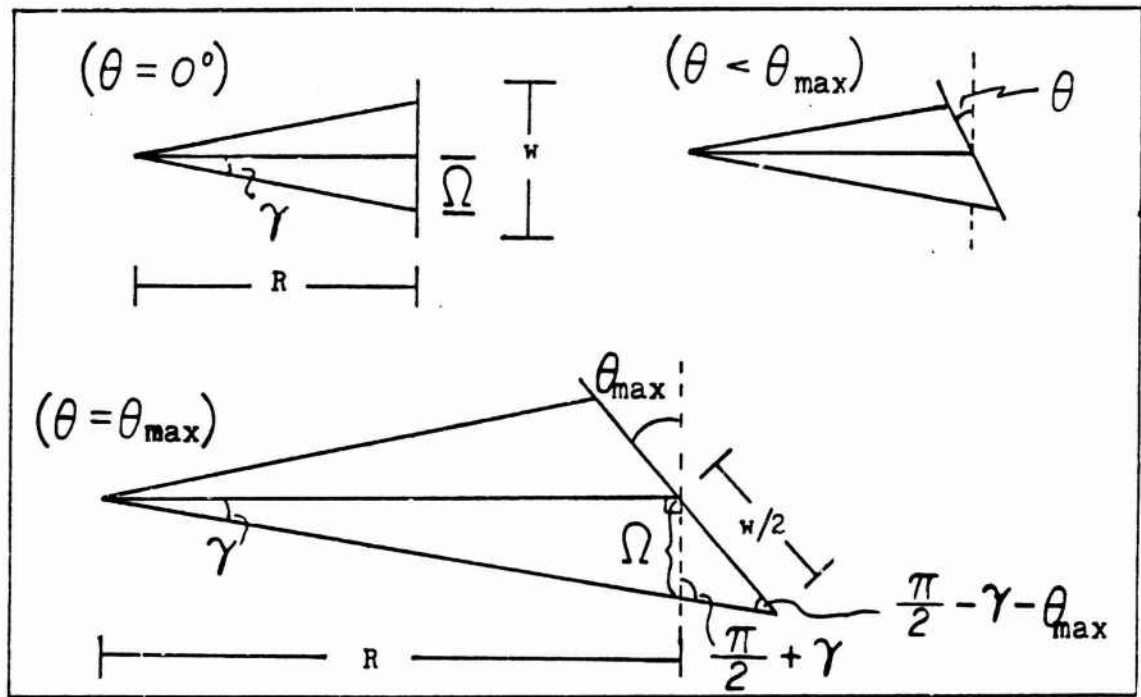
Figure 8. Relationship between R, γ, θ_{max}, and w.

the sample is square and w is sufficiently large, the height of the sample is also sufficiently large. Therefore, the derivation of the relation governing γ in the horizontal and vertical planes, R, A, and θ_{max} can be replaced with the two dimensional problem involving R, γ, θ_{max}, and w. Figure 8 shows the geometry of the relation between R, γ, θ_{max}, and w.

From Figure 8 and the law of sines

$$\frac{\frac{w}{2}}{\sin(\frac{\pi}{2} + \gamma)} = \frac{\Omega}{\sin(\frac{\pi}{2} - \gamma - \theta_{max})} \tag{90}$$

33

$$\frac{w}{2} = \frac{\sin(\frac{\pi}{2} + \gamma)}{\sin(\frac{\pi}{2} - \gamma - \theta_{max})} \Omega \qquad (91)$$

$$= \frac{\cos(\gamma)}{\cos(\gamma + \theta_{max})} \Omega \qquad (92)$$

$$\Omega = R \tan(\gamma) \qquad (93)$$

$$\frac{w}{2} = \frac{R \tan(\gamma) \cos(\gamma)}{\cos(\gamma + \theta_{max})} \qquad (94)$$

$$= \frac{R \sin(\gamma)}{\cos(\gamma + \theta_{max})} \qquad (95)$$

$$R = \frac{w \cos(\gamma + \theta_{max})}{2 \sin(\gamma)} \qquad (96)$$

The maximum R for a given γ (beamwidth corresponding to maximum allowable illumination level on sample holder), w, and θ_{max} is expressed by Eq (96). If R is set, the maximum angle of incidence for choice of γ and w is

34

$$\theta_{max} = \cos^{-1} \left[\frac{2R \sin(\gamma)}{w} \right] - \gamma \qquad (97)$$

To summarize:

1. An increase in R requires a decrease in θ_{max} and/or an increase in w.

2. An increase in θ_{max} requires a decrease in R and/or an increase in w.

   An increase in w requires an increase in R or the planar quality of the incident wave is degraded.

4. Decreasing γ allows for larger θ_{max} , larger R, and smaller samples.

   The sample holder was built to hold samples of size up to 12 in by 12 in and thickness up to 1 1/2 in. For a maximum sample holder illumination of 30 db below the main beam level, the E and H-plane beamwidths are set to 10° and 7° respectively. Pairs of values of R_{max} and θ_{max} are given for both perpendicular and parallel polarization in Table I. In Chapter V the effect of varying R on the measured data will be shown.

   A block diagram of the entire equipment configuration is given in Figure 9. Equipment failures in the receiving subsystem forced the modification of the original set-up (Figure 9.a) to the final equipment set-up (Figure 9.b). The primary component of the system, the antenna support/sample holder assembly, has been described in detail. The remainder of the equipment serves to generate and receive the millimeter wave test signal.

   The essential requirements of the source are frequency and power stability. The source used was a Gunn phase-locked oscillator. The

35

TABLE I

R_{max} versus θ_{max}

	R_{max} (in)	
θ_{max}	Perpendicular ($\gamma = 7°$)	Parallel ($\gamma = 10°$)
50°	26.8	17.3
55°	23.1	14.6
60°	19.2	11.8
65°	15.2	8.9
70°	11.1	6.0

oscillator is locked to a low frequency stable reference signal from a self-contained crystal oscillator.

The receiver subsystem employs harmonic mixing to lower the test frequency to the normal operating range of the receiver. In the original arrangement, the eighth harmonic of an 11.45 GHz local oscillator (LO) was mixed with the 94 GHz test frequency to produce an intermediate frequency (IF) of 2.4 GHz. This IF was filtered and amplified prior to proceeding to the 1783 receiver. In the modified arrangement, the test signal had to be mixed with a harmonic of the receiver's local oscillator. To maximize the received power and therefore the available dynamic range, it was necessary to mix the 94 GHz signal with a harmonic as low in number as possible. The 1783 receiver was replaced with the less sophisticated 1752 receiver because the 1752 had an LO of 1 to 4 GHz,

36
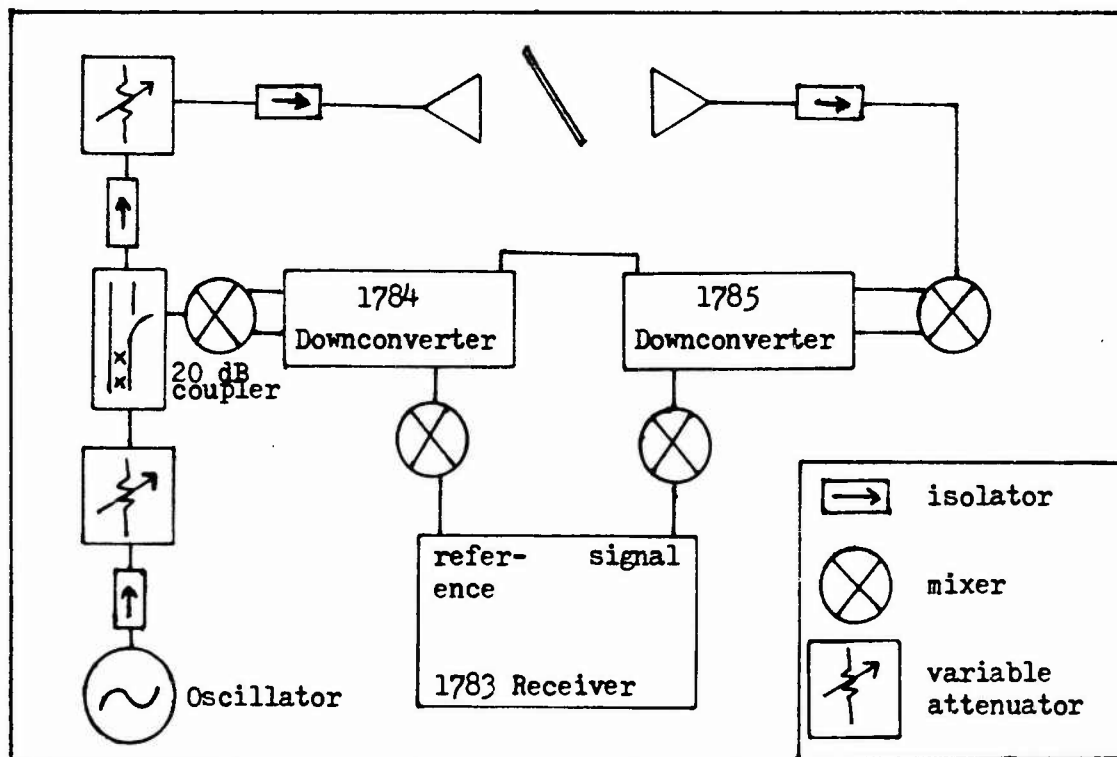
Figure 9.a   Original Equipment Set-Up
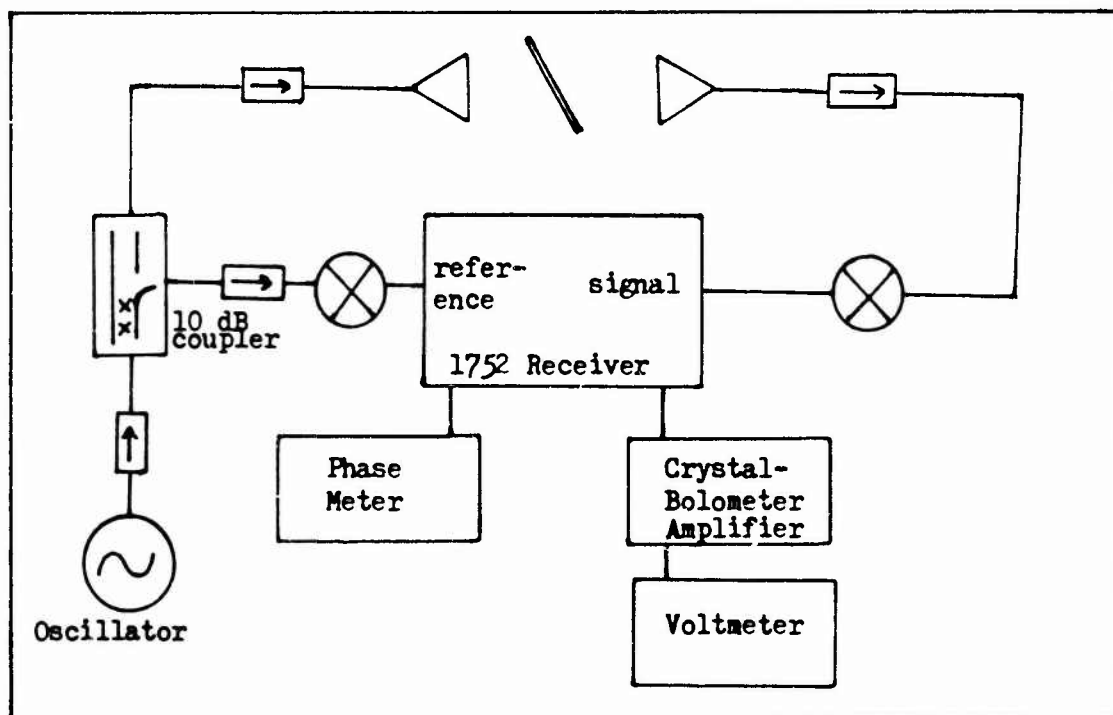
Figure 9.b   Modified Equipment Set-Up

37

which allowed mixing to be accomplished with the twenty-forth harmonic of a 3.917 GHz LO frequency. The LO of the 1783 was limited to 2 GHz, so the 94 GHz test signal had to be mixed with the forty-eighth harmonic of 1.958 GHz. Although the 1783 was able to lock to the test signal, the received power levels were unsuitably low. The attenuators were not included in the modified set-up because the power levels were too low to saturate the mixers or receiver. The isolators were used to minimize reflections in the waveguide components. The 1752 receiver required the use of a voltmeter to obtain amplitude data. Measurement accuracy suffered from this because as the decibel values of power approached -20 to -30 dB for absorber samples, the linear values of voltage decreased by a factor of 10 to 32.

$$(T^2)_{dB} = 10 \log_{10}(\text{power ratio})$$

$$= 20 \log_{10}(\text{voltage ratio})$$

$$\text{voltage ratio} = \log_{10}^{-1} (T^2_{dB}/20)$$

Numerical Solution

The transmission coefficient (T) can be expressed as a function of ϵ', ϵ'', μ', and μ'' with θ_i as a parameter. Solution for the material constants requires four equations, which are obtained by measuring T^2 for at least four distinct values of θ_i, where T^2 is a real quantity representing the magnitude squared of T.

$$\left[T (\epsilon', \epsilon'', \mu', \mu''; \theta_n) \right]^2 = A_n \qquad n=1,2,3,4 \qquad (98)$$

38

where A_n is a constant equal to the magnitude squared of the ratio of the amplitude of the field transmitted through a sample at angle θ_n to the amplitude of the field with no sample present. The numerical method determines the roots to the following system of equations:

$$F_n = \left[T(\epsilon', \epsilon'', \mu', \mu''; \theta_n) \right]^2 - A_n = 0 \quad n=1,2,3,4 \quad (99)$$

The basic operation of the computer code is to calculate the values of T^2_n corresponding to a trial vector of material constants, compare these values to the measured A_n's, and revise the trial vector such that the values of T^2_n move closer to the A_n's. This process continues until the F_n's are within a specified tolerance of zero. The criterion used to compare the current T^2_n's to the A_n's is one of least squares. A function G is defined as the sum of squares of the F_n's.

$$G = \sum_{n=1}^{4} F_n^2 \quad (100)$$

The code attempts to find values of ϵ and μ that minimize G. It is desired that the numerical technique converge to a solution regardless of the initial values. The technique that was chosen is called the method of steepest descent (10:511-517). In this method the trial vector is revised by evaluating the gradient of G at the current values of ϵ and μ and adjusting the trial vector in the direction of the negative gradient. The program continues to revise the trial vector until: (i) the value of G is less than the specified tolerance

39

(ii) there is no improvement from one revision to the next (G does not

decrease)

(iii) the magnitude of the gradient of G is close to zero, or

(iv) the preset maximum number of iterations is exceeded.

There are other techniques that feature faster convergence than the method of steepest descent, but they require close starting approximations to the solution. Although a fairly close approximation to ϵ and μ can usually be made from measurements at other frequencies, it was desired that the numerical solution not depend on prior knowledge of ϵ and μ. If close values are known for the parameters, they can be used as the starting point for the steepest descent technique to speed convergence. If faster convergence is required, the steepest descent technique can be used to obtain a suitable starting approximation for one of the faster techniques.

A program utilizing the steepest descent technique was written for both the case of perpendicular (MUEPSPERP) and parallel (MUEPSPARL) polarization. In Chapter V of this report the two programs are tested and the differences in the results obtained are shown. The expressions for T^2 and the gradient of G are derived in Appendix B.

Although MUEPSPERP and MUEPSPARL are written for materials of arbitrary ϵ and μ, it will be shown in Section V that it is advantageous to use specialized programs for materials that are considered to be pure dielectrics or for materials that are considered to be nonmagnetic. The programs NONMAGPERP and NONMAGPARL are specialized versions of MUEPSPERP and MUEPSPARL. The substitution $\mu = \mu_0$ has been made and T^2 is considered to be a function of ϵ', ϵ'', and the parameter θ only.

40

These programs require only two angles of incidence since there are only two unknowns.

For the case of pure dielectrics, the only unknown is ϵ' and the method of steepest descent is not needed. The programs PURDIELPERP and PURDIELPARL calculate a value of ϵ' for each pair of values θ and A. These programs utilize a subprogram ZEROIN (11:161-166) which determines a root to a function of one variable by taking an interval that contains a root and successively decreasing the size of the interval until it is smaller than a preset tolerance value. At this point one of the endpoints of the interval is output as the root of the equation. The program must be given a starting interval which contains the root of the equation. It will be seen in Chapter V that the equation for T^2 as a function of ϵ' has multiple roots. The correct solution in this case requires that an interval containing only the desired root be given as the starting interval. In Chapter V a method of determining an appropriate starting interval is discussed.

V. Testing and Evaluation

The measurement system is divided into two parts, the computer code that calculates ϵ and μ from measured values of T^2 and the equipment that is used to measure T^2. Since comparable data for absorber materials at 94 GHz is not available, the two parts of the system are first tested separately under known conditions. The codes are tested by entering calculated values of T^2 for a hypothetical material of given ϵ and μ and comparing the material constants derived by the code to the given constants. The measurement of T^2 is evaluated by measuring a known sample of plexiglass. Finally, results obtained for a sample of nonmagnetic absorber and a sample of magnetic absorber are presented together with data obtained at microwave frequencies by other techniques.

Testing of Codes

General Materials. The computer code underwent several modifications and results obtained by the different versions are compared. For convenience, the following vectors are defined:

$\underline{X}_a$: the actual material constants,

$$\underline{X}_a = [\epsilon', \epsilon'', \mu', \mu'']$$

$\underline{X}_i$: the initial values chosen for the material constants,

$\underline{X}_f$: the final vector produced by the code,

$\underline{A}$: the vector of angles used in a particular example,

42

$\underline{T}_m$: the vector of T^2 corresponding to $\underline{X}_a$ and $\underline{A}$,

$\underline{T}_f$: the vector of T^2 corresponding to $\underline{X}_f$ and $\underline{A}$.

For the testing of the codes, theoretical values are used for $\underline{T}_m$.

The original code was written to solve the system of equations

$$F_n = \left[T(\epsilon', \epsilon'', \mu', \mu''; \theta_n) \right]^2 - A_n = 0 \quad n=1,2,3,4 \quad (99)$$

for any material whose constants could be written in the form

$$\epsilon = \epsilon' - j\epsilon'' \quad (13)$$

$$\mu = \mu' - j\mu'' \quad (20)$$

The inputs to the programs are the test frequency, sample thickness, $\underline{A}$, and $\underline{T}_m$. A separate code was written for the cases of perpendicular and parallel polarization of the incident wave. For the purpose of illustration, the results are shown for a material with constants $\underline{X}_a = [5, 1, 2, 1]$ and thickness of 100 mils at angles $\underline{A} = [0°, 20°, 40°, 60°]$ and a frequency of 94 GHz. The initial values are chosen to be $\underline{X}_i = [4, 0.5, 1, 0.5]$. The results are judged by comparing the material constants derived by the code $(\underline{X}_f)$ to the given values $(\underline{X}_a)$ and by comparing the values of T^2 $(\underline{T}_f$ and $\underline{T}_m)$ that correspond to $\underline{X}_f$ and $\underline{X}_a$.

The results obtained by the original codes are shown in Table II. Although the values of T^2 agree fairly well ($\underline{T}_f$ is close to $\underline{T}_a$), the derived material constants are not close to the actual ones. Given

43

TABLE II

Results Obtained with Original Codes

Polarization	$\underline{X}_f$	$\underline{T}_f$	$\underline{T}_m$	G
Perpendicular	4.178	47.956	47.960	
	0.535	48.330	48.318	8.7×10^{-15}
	1.927	49.466	49.426	
	1.297	51.668	51.660	
Parallel	5.041	47.957	47.960	
	0.569	48.118	48.108	1.0×10^{-14}
	1.693	48.560	48.524	
	1.120	49.385	49.356	

enough iterations, the codes should converge to $\underline{X}_a$ but there are practical difficulties associated with using the method of steepest descent to solve Eq (99).

Since $T^2 \leq 1$, the error term G can never be greater than 4 and will typically be much less than 1 for lossy samples. For the example considered here, each element of $\underline{T}_m$ is on the order of 10^{-5}. When $\underline{T}_c$ is subtracted from $\underline{T}_m$ and the difference squared, G becomes small quickly. To increase the magnitude of G it was decided to express T^2 in decibel form:

$$T^2_{dB} = 10 \log_{10}(T^2)$$

44

TABLE III

Results Obtained with Final Codes

Polarization	X_f	T_f	T_m	G
Perpendicular	4.215	47.956	47.960	
	0.534	48.329	48.318	8.6×10^{-4}
	1.933	49.460	49.426	
	1.294	51.659	51.660	
Parallel	5.064	47.957	47.960	
	0.547	48.107	48.108	1.6×10^{-5}
	1.839	48.526	48.524	
	1.163	49.353	49.356	

Another difficulty with solving Eq (99) is the number of arithmetic calculations required to determine the gradient of G (Appendix B). The number of iterations that can be used before G stops decreasing is limited by the accumulation of round-off error. To reduce the round-off error the codes were converted to double precision FORTRAN. The final version of the codes (MUEPSPERP and MUEPSPARL) are the double precision versions with T^2 expressed in decibels. The results obtained by these versions for the hypothetical material are given in Table III.

The results have improved but are still not satisfactory. It was observed that MUEPSPERP consistently produced better solutions for ϵ'' and μ' and MUEPSPARL consistently produced better solutions for ϵ' and μ''. To demonstrate this explicitly, results are given for an example with $\epsilon = \mu$ in Table IV. The reason for this behavior is the different

TABLE IV

Example: $\epsilon = \mu$

$\underline{X}_a$	$\underline{X}_i$	$\underline{X}_f$	
		MUEPSPERP	MUEPSPARL
2.0	1	1.581	2.084
0.2	1	0.237	0.144
2.0	1	2.084	1.580
0.2	1	0.145	0.237

TABLE V

Results Obtained with Sequence of MUEPSPERP and MUEPSPARL

$\underline{X}_f$	Perpendicular		Parallel	
	$\underline{T}_f$	$\underline{T}_m$	$\underline{T}_f$	$\underline{T}_m$
5.066	47.975	47.960	47.975	47.960
0.541	48.333	48.318	48.121	48.108
1.918	49.441	49.426	48.533	48.524
1.185	51.676	51.660	49.365	49.356

functional dependence of T^2 on each of the four material parameters for the two different polarizations. The parameter by which the partial derivative of T^2 is greatest dominates the gradient of G and therefore the code concentrates primarily on improving the value of that parameter. In an attempt to improve the derived material constants $\underline{X}_f$ by using

46

the equations for both the perpendicular and parallel cases, the corre-
sponding codes were run iteratively with the output $\underline{X}_f$ produced by one
code used as the input $\underline{X}_i$ for the other. This approach, although cum-
bersome, yields a satisfactory $\underline{X}_f$. Also, if the $\underline{X}_f$ obtained is such
that the corresponding values of T^2 ($\underline{T}_f$) closely approximate the meas-
ured values ($\underline{T}_m$) for both polarizations, the confidence that the derived
constants are close to $\underline{X}_a$ is increased. The results obtained by running
the two codes in sequence once are given in Table V. $\underline{X}_f$ can be improved
further by continuing the iterative substitution process.

Nonmagnetic Materials. The programs for nonmagnetic materials are
the final versions of the general programs with the substitution made
that $\mu = \mu_0$ and the derivatives with respect to μ' and μ'' removed.
Since the measurement of T^2 is limited to four significant figures, it
is important to examine the performance of the codes when $\underline{T}_m$ is known to
four significant figures. The codes are also tested by assuming a 5%
error in the measured values. The results obtained for these cases are
summarized in Table VI.

Pure Dielectrics. Although the main application of this system is
not to measure pure dielectrics, it was done to verify the ability to
accurately measure the transmission coefficient. This cannot be veri-
fied with absorber materials directly because comparative data from
other systems is not available above 26 GHz. Since the codes developed
to determine ϵ and μ for lossy materials do not work well for lossless
r erials, a separate code for pure dielectrics was written.

T^2 is a function of only one variable (ϵ') in this case, thus it
can be graphed versus ϵ' for a given frequency, sample thickness, angle

47

TABLE VI

Results Obtained with Codes for Nonmagnetic Materials

Code		X_f		
		4 sig. figures	+ 5% error	- 5% error
NONMAGPERP	2.000	2.006	1.984	1.985
	2.000	2.002	1.972	2.017
NONMAGPARL	2.000	1.991	1.988	1.994
	2.000	1.997	1.974	2.021
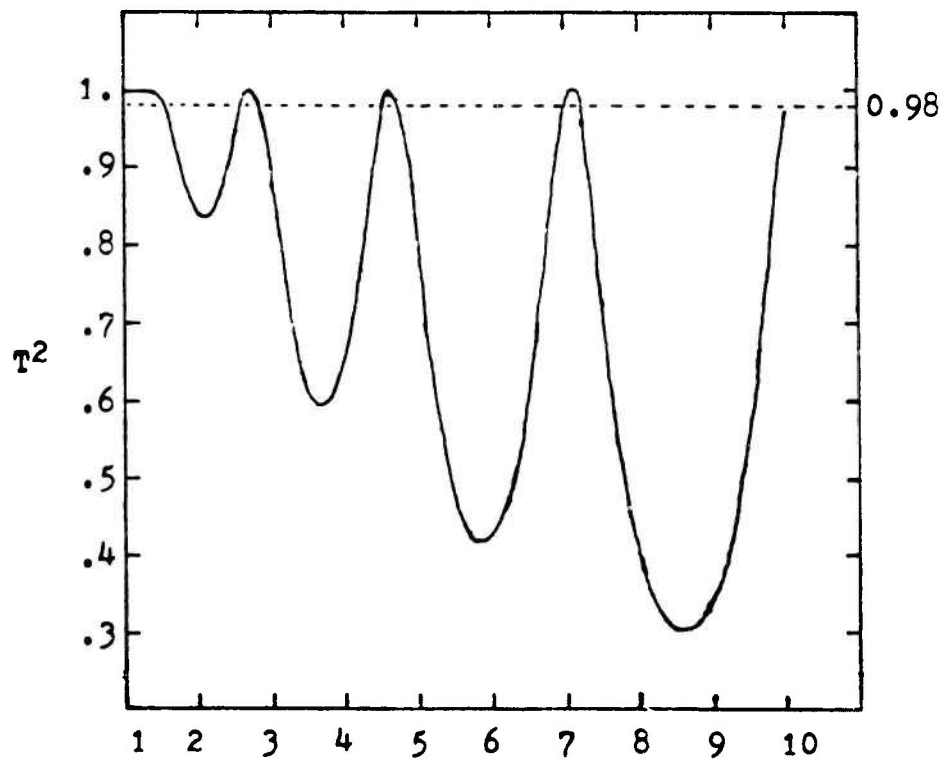
Figure 10. T^2 versus Permittivity for Pure Dielectrics

48
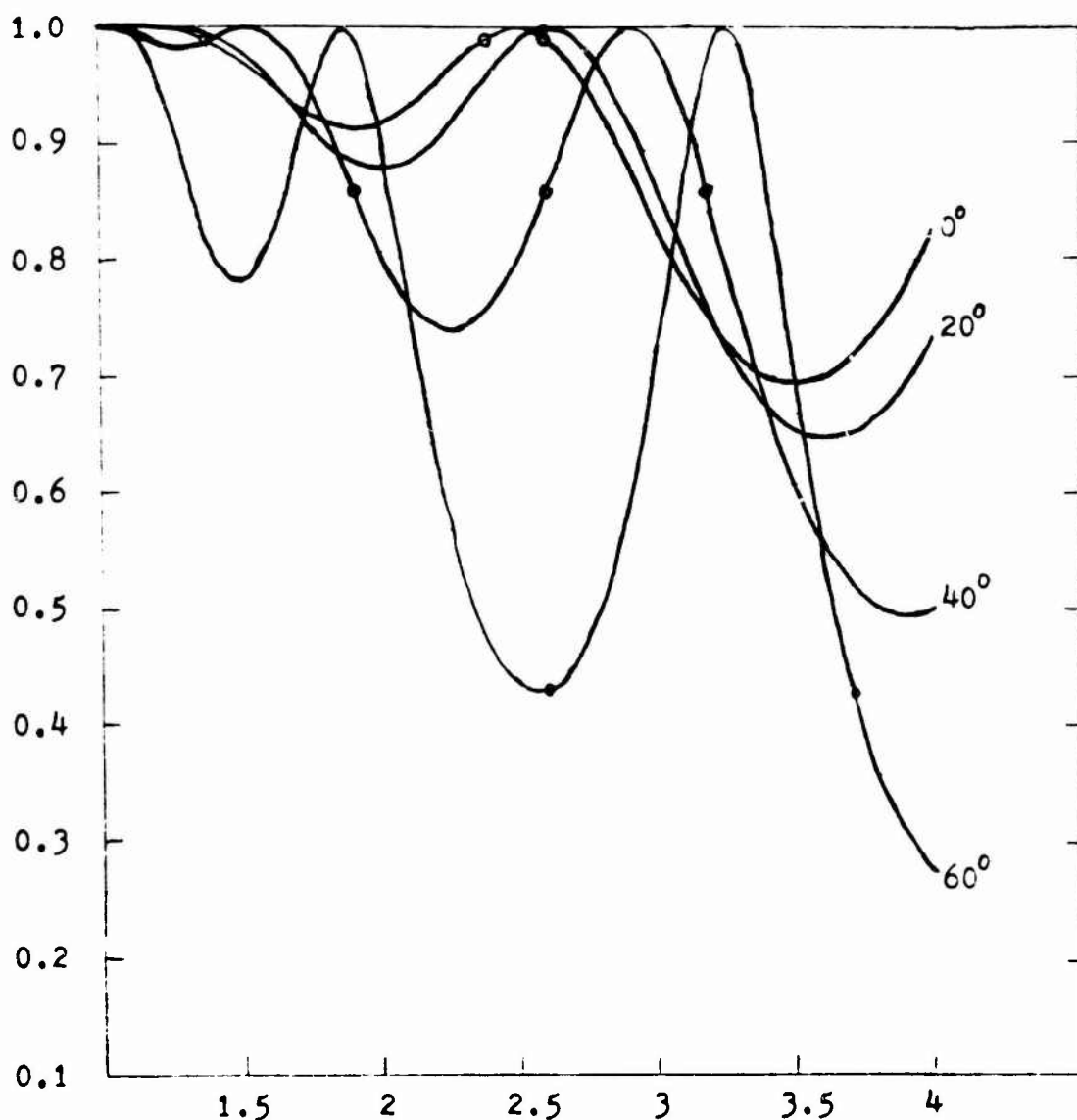
Figure 11. T^2 versus ϵ' for Several Angles of Incidence

of incidence, and polarization. Such a graph is given in Figure 10 for ϵ' ranging from 1 to 10. It is seen that T^2 is not a singular function, that is ,given a value of T^2, there is not a unique ϵ'. If one knows an interval that contains a unique value of T^2, then the corresponding ϵ' can be uniquely determined. For example, in Figure 10, $T^2 = 0.98$ has seven roots for the interval (1,10). Given the following intervals,

(1,2), (2,2.7), (2.7,4), (4,4.6), (4.6,6), (6,7.1), and (7.1,10);
PURDIELPERP identifies the roots as 1.543, 2.589, 2.829, 4.529, 4.728,
6.700, and 7.185. A suitable interval can usually be identified from
known results at other frequencies since ϵ' is not a strong function of
frequency for lossless materials. If the measured T^2 happens to fall
near a critical point of the graph, there will be two possible roots
close to each other. To determine the correct root, data can be taken
at another angle and the value of ϵ' that is a root for both angles is
chosen to be correct. Figure 11 shows how the curve of T^2 versus ϵ'
varies as the angle of incidence is changed. The critical points at one
angle appear at different values of ϵ' at another angle. For example,
consider a sample of thickness 119 mils being illuminated by a 94 GHz,
perpendicularly polarized waveform. If the measured values of T^2 are

$$
\begin{array}{lll}
0.99 & \text{at} & 0° \\
1.00 & \text{at} & 20° \\
0.86 & \text{at} & 40° \\
\text{and} \qquad 0.44 & \text{at} & 60°
\end{array}
$$

then $\epsilon' = 2.6$ is the only root that satisfies more than one of the
measurements. The effect of measurement error on the determination of ϵ'
depends on the instantaneous slope of the curve of T^2 versus ϵ'.
Therefore, the error in ϵ' for a given error in T^2 differs considerably
for different operating conditions, such as angle of incidence, sample
thickness, polarization, and frequency.

Measurement of T^2

The ability to measure T^2 and the influence of the sample-to-
antenna distance R were investigated by taking data on a sheet of

TABLE VII

Permittivity of Plexiglass

θ_i	R:	Perpendicular							Parallel
		3	4	5	6	7	9	11	11
0		2.58	2.60	2.64	2.64	2.61	2.63	2.63	2.60
5		2.59	2.64	2.69	2.69	2.64	2.62	2.65	2.59
10		2.61	2.66	2.68	2.71	2.65	2.64	2.67	2.61
15		2.64	2.69	2.71	2.74	2.68	2.67	2.69	2.64
20		2.55	2.50	2.47	2.44	2.50	2.52	2.51	2.69
25		2.60	2.57	2.50	2.52	2.57	2.60	2.58	2.59
30		2.71	2.65	2.55	2.63	2.65	2.67	2.64	2.64
35		2.79	2.73	2.59	2.75	2.73	2.74	2.70	2.70
40		2.92	2.82	2.66	2.87	2.80	2.81	2.74	2.75

plexiglass. The permittivity of plexiglass is expected to be very close
to 2.6 at millimeter wavelengths (12:334). Data was taken in 5° incre-
ments for distances of 3 to 11 inches and is presented in Tables VII and
VIII. The mean of the data is approximately equal as R is varied, but
the standard deviation decreases as R is increased to 11 inches. It is
believed that this can be attributed to the greater interference between
the sample and antennae for smaller R and to the improvement in the
planar quality of the incident wave as R increases. The sponsoring
laboratory has taken data on plexiglass on both its time domain system
and its network analyzer system. The data from the two systems agree

TABLE VIII

Mean and Standard Deviation of Plexiglass Permittivity Data

	Perpendicular							Parallel
R(in) :	3	4	5	6	7	9	11	11
Mean 0°-30°	2.61	2.62	2.61	2.62	2.61	2.62	2.62	2.62
Mean 0°-35°	2.63	2.63	2.60	2.64	2.63	2.64	2.63	2.63
Mean 0°-40°	2.67	2.65	2.61	2.67	2.65	2.66	2.65	2.65
Std. Dev. 0°-40°	0.34	0.27	0.25	0.36	0.25	0.24	0.19	0.16

well; the network analyzer data is presented in Figure 12.

Absorber Data

It was decided to set R equal to 11 inches for the measurement of absorber and to take data in 3° increments ranging from 9° to 36° . The angles near normal incidence were not used because of reflections between the sample and antennae. This choice yields 10 data points, which is sufficient for the numerical solution. The use of a smaller R and greater range of angles is rejected because the reflection from samples of absorber is typically greater than that of the plexiglass sample and the interference will be worsened.

Nonmagnetic Absorber. The material chosen to measure was Eccosorb LS-24. The sponsoring laboratory has measured this material also on the
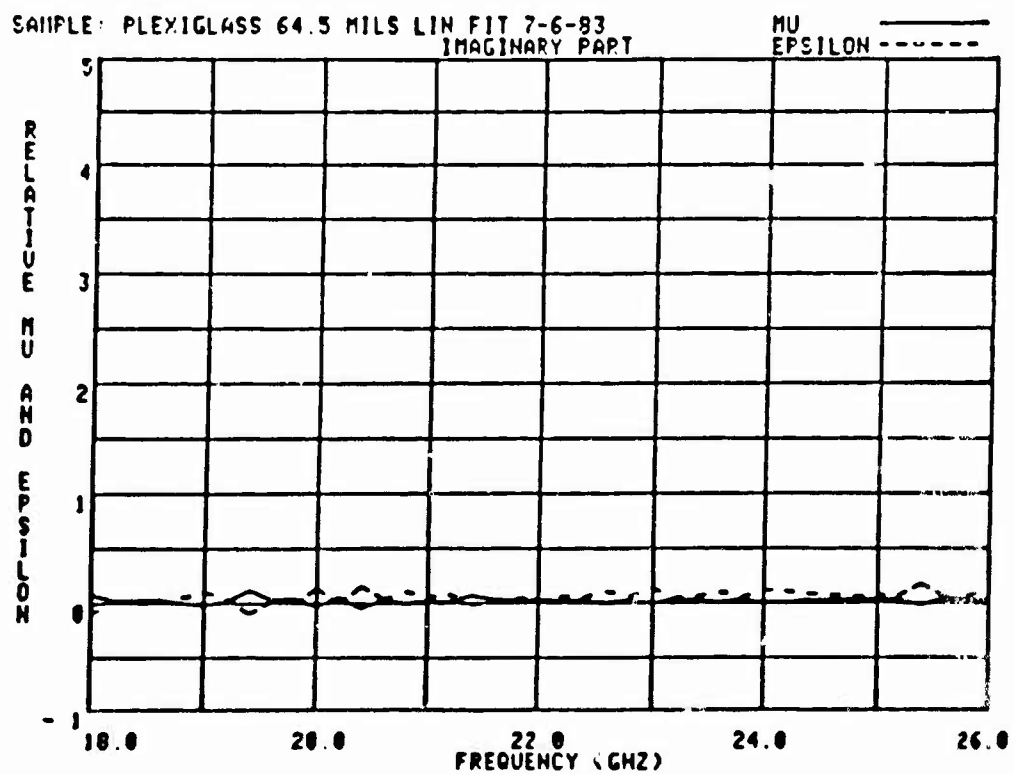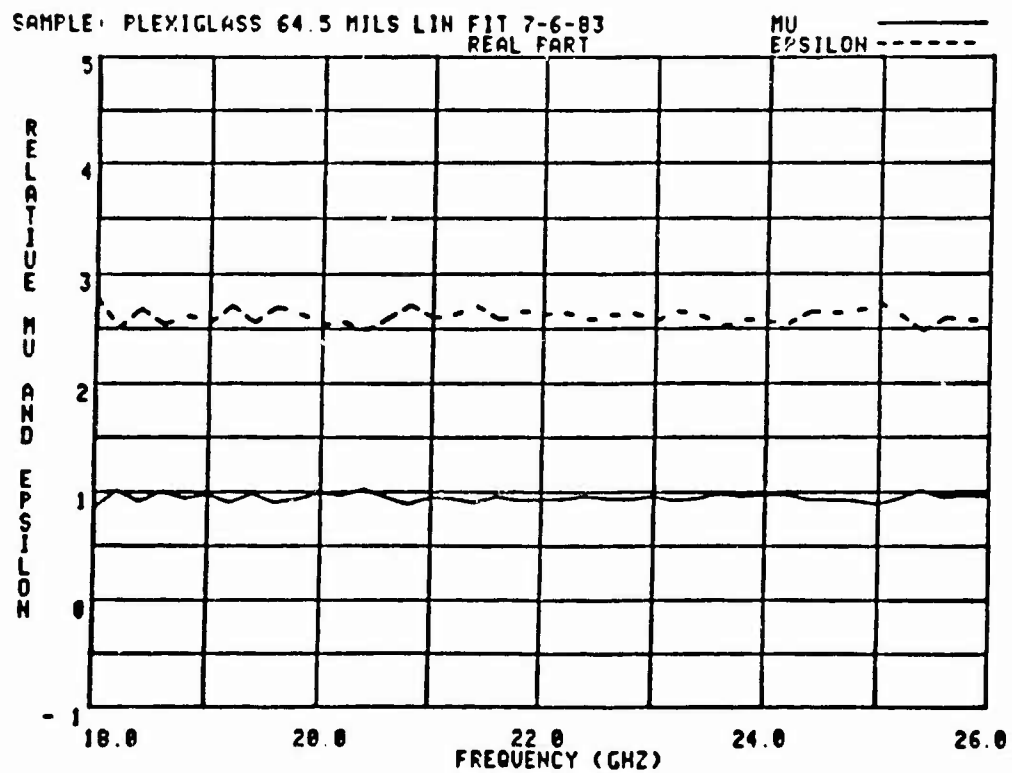
SAMPLE: PLEXIGLASS 64.5 MILS LIN FIT 7-6-83   MU ————
                    REAL PART   EPSILON - - - - -

Figure 12. Mu and Epsilon of Plexiglass (Network Analyzer) (13:44)

53

TABLE IX

LS-24 Data

Parallel Polarization			
Angles	ϵ'	ϵ''	G
9°, 30°	0.951	0.378	2.0×10^{-17}
15°, 36°	1.06	0.401	1.7×10^{-16}
12°, 24°	0.928	0.373	3.5×10^{-15}
9°, 24°	0.929	0.374	6.7×10^{-16}
12°, 27°	0.943	0.376	4.1×10^{-15}
15°, 30°	0.982	0.386	8.2×10^{-18}
18°, 33°	1.02	0.396	2.4×10^{-15}
21°, 36°	1.11	0.415	2.7×10^{-16}
18°, 30°	1.02	0.394	1.3×10^{-15}
21°, 33°	1.04	0.400	5.1×10^{-16}

Perpendicular Polarization			
Angles	ϵ'	ϵ''	G
9°, 30°	1.44	0.533	3.4×10^{-16}
9°, 21°	1.49	0.541	3.3×10^{-13}
12°, 24°	1.51	0.545	1.5×10^{-13}
15°, 27°	1.31	0.510	1.3×10^{-15}
18°, 30°	1.56	0.555	1.3×10^{-15}
12°, 27°	1.36	0.518	2.5×10^{-15}
15°, 21°	1.51	0.544	2.5×10^{-15}
18°, 24°	1.53	0.548	2.0×10^{-15}

TABLE X

$\underline{T}_f$ Compared to $\underline{T}_m$ for LS-24

	Parallel		Perpendicular	
Angle	$\underline{T}_m$	$\underline{T}_f$	$\underline{T}_m$	$\underline{T}_f$
9°	12.06	12.12	13.86	13.92
12°	12.18	12.24	14.02	14.01
15°	12.38	12.38	14.14	14.13
18°	12.61	12.57	14.25	14.27
21°	12.85	12.79	14.43	14.44
24°	13.06	13.05	14.60	14.63
27°	13.37	13.36	14.85	14.86
30°	13.73	13.71	15.10	15.11
33°	14.11	14.11	-----	-----
36°	14.40	14.57	-----	-----

time domain and network analyzer systems. The results obtained for various pairs of data points are presented in Table IX. The values of permittivity obtained by averaging the individual results are

$$\epsilon = 0.998 - j\ 0.389 \qquad \text{(Parallel)}$$

$$\epsilon = 1.46 - j\ 0.537 \qquad \text{(Perpendicular)}$$

The $\underline{T}_f$ corresponding to these averaged values is compared to $\underline{T}_m$ in Table

X. The discrepancy in the results between the perpendicular and parallel cases is believed to be due primarily to measurement error in T^2 for the perpendicular data. The parallel data was measured with a new voltmeter that was more accurate than the original meter used for the perpendicular data. Time did not permit reconfiguring the equipment to remeasure the perpendicular data. Data from the network analyzer system is presented in Figure 13.

Magnetic Absorber. The material chosen to measure was FGM-40. The values of and were arrived at by running the pair of codes MUEPSPARL and MUEPSPERP 25 times. The final values produced by the codes were

$$\epsilon = 19.887 - j\,2.555$$
$$\mu = 0.851 - j\,0.0423$$
(Parallel)

$$\epsilon = 19.900 - j\,2.558$$
$$\mu = 0.833 - j\,0.00138$$
(Perpendicular)

The values of T^2 ($\underline{T}_f$) corresponding to the derived material constants are compared to the measured values ($\underline{T}_m$) in Table XI. The codes took so long to converge because μ turned out to be very close to μ_o. Data from the network analyzer system was not available for FGM-40; data obtained by the time domain system is presented in Figure 14 for comparison to the results obtained here.
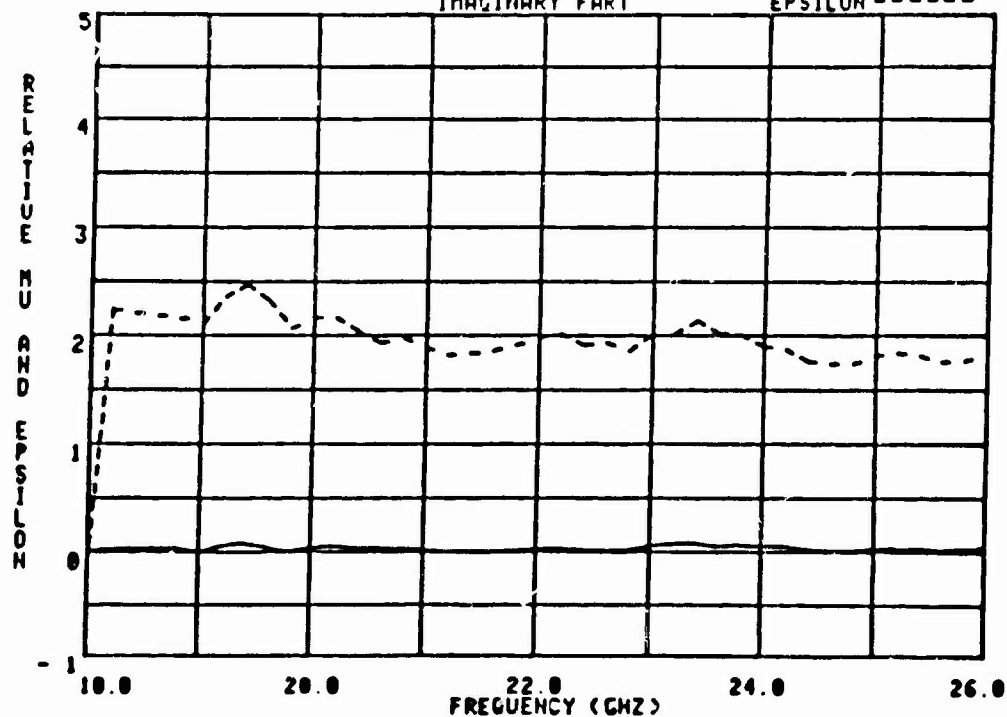
56
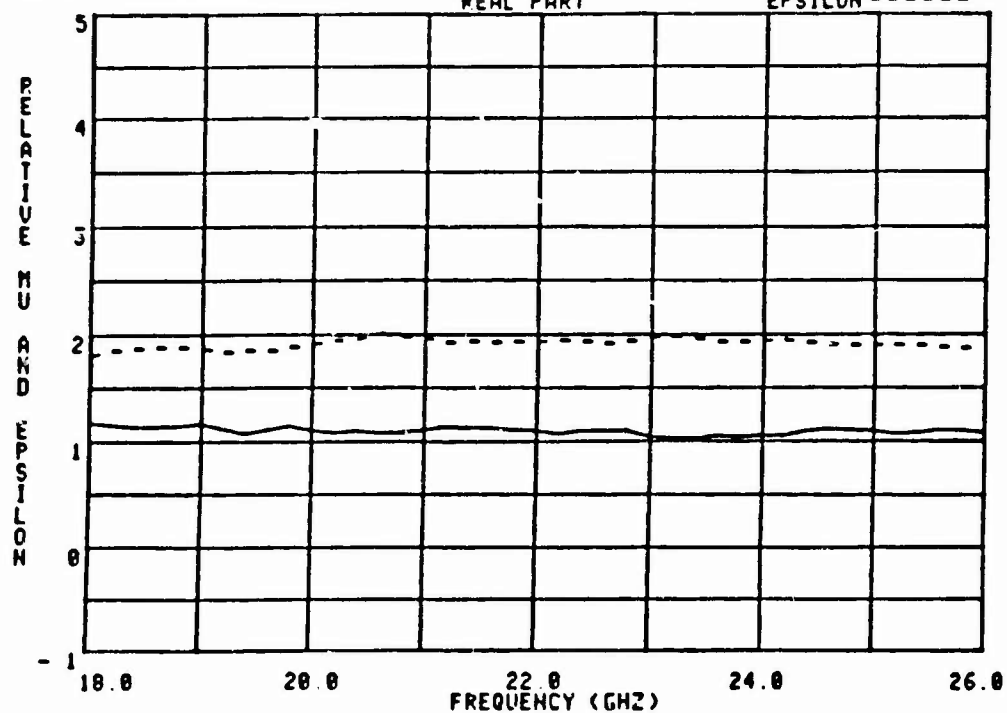
Figure 13.   Mu and Epsilon of LS-24 (Network Analyzer) (13:53)

TABLE XI

$\underline{T}_f$ Compared to $\underline{T}_m$ for FGM-40

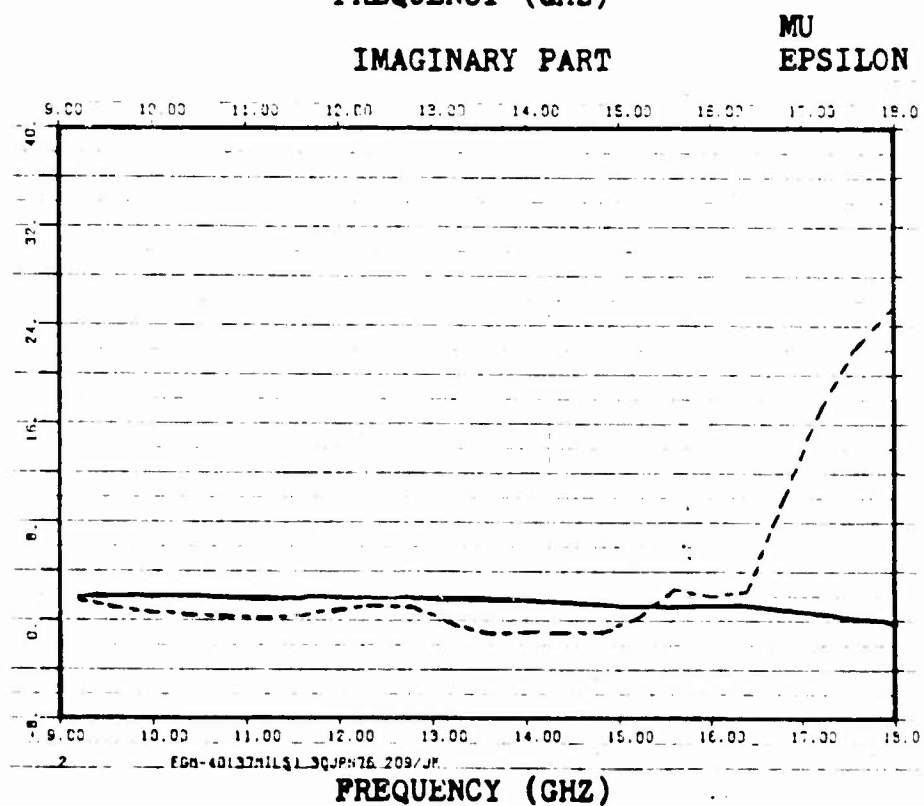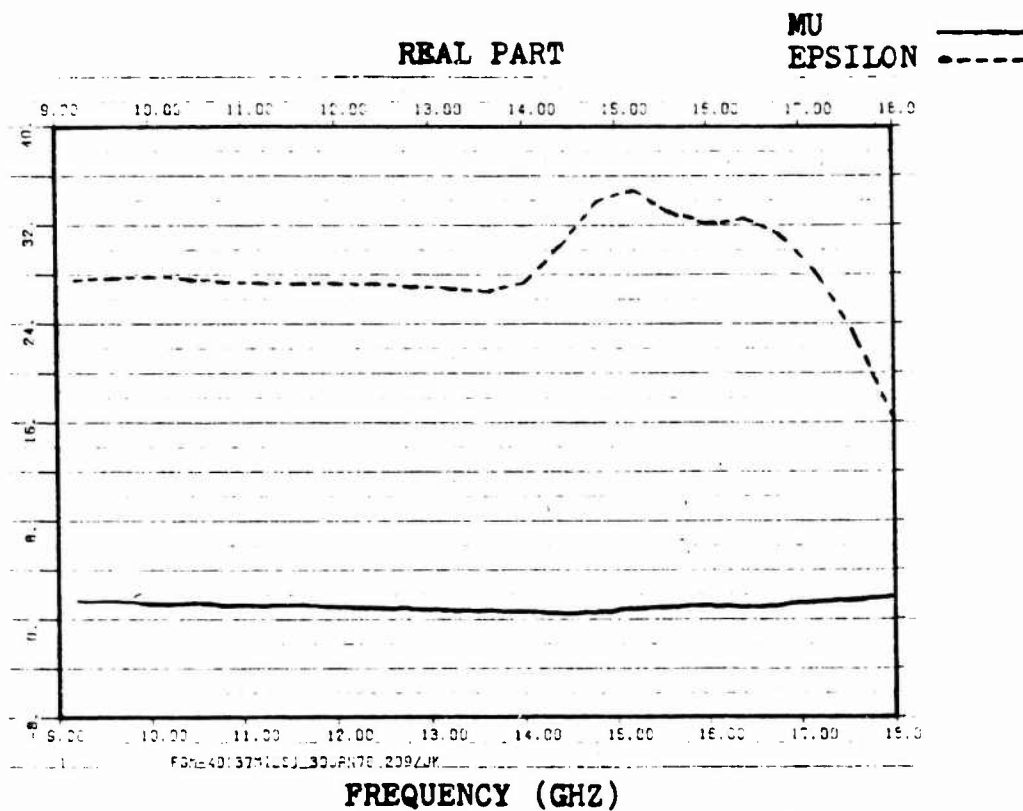|	Parallel		Perpendicular	
Angle	$\underline{T}_m$	$\underline{T}_f$	$\underline{T}_m$	$\underline{T}_f$
9°	11.83	11.83	10.58	10.59
12°	11.80	11.78	10.62	10.66
15°	11.73	11.72	10.75	10.75
18°	11.64	11.64	10.87	10.86
21°	11.56	11.55	11.04	10.99
24°	11.44	11.43	11.17	11.15
27°	11.31	11.31	11.30	11.33
30°	11.15	11.16	11.52	11.53
33°	11.00	11.00	-----	-----
36°	10.81	10.81	-----	-----

Figure 14. Mu and Epsilon for FGM-40 (Time Domain System)

VI. Conclusions and Recommendations

This thesis included the design of both a technique of measuring permittivity and permeability and the equipment needed to implement the technique. A test system was produced and used to measure several representative materials. This chapter presents conclusions about the measurement system and makes recommendations regarding further development of the system.

As a result of the experimentation performed in this thesis, the following is concluded:

1. The permittivity and permeability of lossy, linear, homogeneous, isotropic materials can be determined from measurement of the magnitude of the transmission coefficient of a planar sample at a minimum of four angles of incidence.

2. Data taken under both perpendicular and parallel polarization of the incident wave is necessary to insure good results for materials of general ϵ and μ.

3. Two data points from either polarization are sufficient for materials that can be assumed to be nonmagnetic; the measurement system performs well for such materials.

4. The codes do not yield good results for very low loss materials, but it is believed that with further modification the results for such materials can be improved. A separate code to determine the permittivity of pure dielectrics has been developed here and yields satisfactory results.

60

5. The transmission coefficient can be measured at distances much shorter than that prescribed by the far field criterion by using antennae fitted with lenses. Also, the need to enclose the measurement apparatus in an anechoic chamber can be eliminated by the use of narrow beamwidth antennae.

As a continuation of this research effort, the following is recommended:

1. Since the number of calculations needed for the gradient of G appears to be limiting the numerical solution, replace the exact expressions for the partial derivatives with a numerical differentiation routine.

2. The expression for the magnitude of the transmission coefficient is considerably more complicated than that of the transmission coefficient, yet the latter is a complex quantity. Since the equipment has the capability to measure the phase of the transmission coefficient, the system could likely be improved by developing a numerical solution that solves for complex roots and uses the phase measurements.

3. As opposed to the present approach of a system of four equations in four unknowns, nonlinear regression may be used. Such a technique would have the advantage of utilizing all the data points at once.

4. Other numerical techniques that feature faster convergence than the method of steepest descent may be investigated. As a first step, it may be desirable to use the steepest descent method with one set of data points to obtain a suitable starting approximation and then use a faster technique for the remainder of the data.

5. Since the system now requires both perpendicular and parallel data for general materials, it would be an improvement to have a single code that utilizes both types of data. One possibility is a code with four equations, two perpendicular and two parallel, taken from the present codes. Another possibility is to use the two present codes as subroutines in a program that would alternate between the two subroutines, using the output of one as the input to the other. If this approach is followed, it would be useful to examine the influence of the number of iterations within each subroutine in relation to the number of times the main program calls the subroutines.

Finally, modifications to the existing equipment could enhance the performance of the measurement system. Specifically, the following recommendations are made:

1. Obtain a sample holder that can be rotated about a horizontal axis as well as a vertical axis. This would allow data to be taken under both polarizations without rotating the antennae. An alternative to this is to obtain equipment that would allow for the polarization to be changed electrically.

2. Develop the equipment so that measurements can be made at more than one frequency. With the addition of a network analyzer and a computer-controllable positioner, the system could be automated. Data would be taken and stored for each frequency at one angle, then the sample would be rotated and the process continued.

3. Experiment with increasing the antenna to sample distance to beyond 11 inches.

4. Fasten the sample holder/positioner and waveguide components

rigidly to a support to eliminate vibrations.

     5.   Construct the sample holder out of a sturdier material.

     6.   Use the original receiver equipment intended for this thesis.

     In the course of developing this material measurement system, several unique characteristics were experimentally verified. First of all, measurements were made at a frequency substantially higher than possible by currently available systems. Secondly, it was shown that transmission could be measured in free space at very short ranges without a shielded enclosure by using horn antennae fitted with dielectric lenses. Finally, a computer code was written that features global convergence to the material constants when given the magnitude of the transmission coefficient at four angles of incidence.

     This thesis project has demonstrated the viability of the above measurement approach and demonstrated that the approach is worthy of further study. The system can be improved and extended in many ways, however the most pressing needs are to continue to modify the computer code, increase the range of frequencies at which measurements can be made, and automate the system.
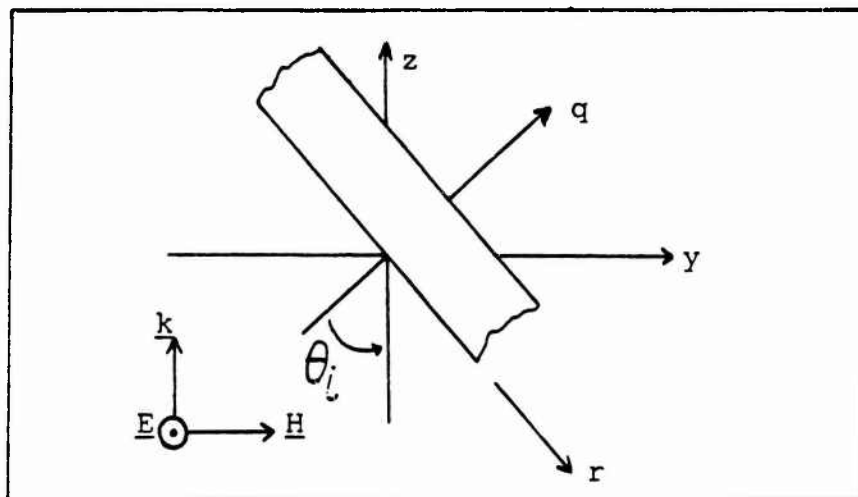
Figure 15. Geometry for Perpendicular Polarization

The derivations presented here follow material given in (2:87-90).

Wave Impedance

Perpendicular Polarization. The incident wave is given by $x E_x$, $y H_y$; where

$$\underline{E}_i = \hat{x} \, E_{ix} \tag{101}$$

$$\underline{H}_i = \hat{y} \, H_{iy} \tag{102}$$

64

$$E_{ix} = e^{-(jk_o z)} \qquad (103)$$

$$H_{iy} = (\frac{\epsilon_o}{\mu_o})^{\frac{1}{2}} e^{-(jk_o z)} \qquad (104)$$

It is convenient to define a coordinate system with one axis parallel to the face of the sheet (r) and one axis normal to the sheet (q). The incident wave can be considered to be a uniform plane wave in the xy plane propagating in the z direction or as a nonuniform wave in the qr frame propagating in the q direction. The xyz and xqr coordinate frames are related by the coordinate transformation

$$x = x \qquad (105)$$

$$y = r \cos(\theta_i) + q \sin(\theta_i) \qquad (106)$$

$$z = -r \sin(\theta_i) + q \cos(\theta_i) \qquad (107)$$

In the xqr frame, the incident field is given by

$$\underline{E}_i = \hat{x} \exp\left[- j k_o \left[-r \sin(\theta_i) + q \cos(\theta_i)\right]\right] \qquad (108)$$

H_i can be determined from $\quad curl \ (\underline{E}) = -jw\mu_o \ \underline{H}$

$$\underline{H}_i = \frac{j}{w\mu_o} curl \ (\underline{E}_i) \qquad (109)$$

65

$$\text{curl} \, (\underline{E}_i) = \hat{r} \left[\frac{\partial}{\partial q} (\underline{E}_{ix}) \right] - \hat{q} \left[\frac{\partial}{\partial r} (E_{ix}) \right] \tag{110}$$

since $E_q = E_r = 0$.

$$\underline{H}_i = \frac{j}{\omega \mu_o} \left[\hat{r} \left[\frac{\partial}{\partial q} (E_{ix}) \right] - \hat{q} \left[\frac{\partial}{\partial q} (E_{ix}) \right] \right] \tag{111}$$

$$= \frac{j}{\omega \mu_o} \left[\hat{r} [-j \, k_o \, \cos(\theta_i)] - \hat{q} [j \, k_o \, \sin(\theta_i)] \right] E_{ix} \tag{112}$$

$$= \frac{k_o}{\omega \mu_o} \left[\hat{r} \, \cos(\theta_i) + \hat{q} \, \sin(\theta_i) \right] E_{ix} \tag{113}$$

Wave Impedance of Free Space. Denote the wave impedance
outside the sample in the direction of increasing q by Z_o. Then

$$Z_o = \frac{E_{ix}}{H_{ir}} \tag{114}$$

$$= \frac{E_{ix}}{(\frac{k_o}{\omega \mu_o}) \, E_{ix} \, \cos(\theta_i)} \tag{115}$$

$$\frac{k_o}{\omega \mu_o} = (\frac{\epsilon_o}{\mu_o})^{\frac{1}{2}} \tag{116}$$

$$Z_o = (\frac{\mu_o}{\epsilon_o})^{\frac{1}{2}} \, \sec(\theta_i) \tag{117}$$

Wave Impedance of the Sample. The wavenumber within the
sheet, k_m, is given by

66

$$k_m = \omega(\mu \, \epsilon)^{\frac{1}{2}} \tag{118}$$

$$= \omega(\mu_r\mu_o \, \epsilon_r\epsilon_o)^{\frac{1}{2}} \tag{119}$$

$$= k_o \, (\mu_r \, \epsilon_r)^{\frac{1}{2}} \tag{120}$$

The incident wave is refracted upon passage through the air/sample boundary and propagates at an angle θ_r to the surface normal. The form of the wave inside the sample is the same as that of the incident wave with θ_i replaced by θ_r and k_0 replaced by k_m. Thus

$$\underline{E}_m^+ = \hat{x} \, E_{mx}^+ \tag{121}$$

$$= \hat{x} \, \exp \left[- jk_m[- r \sin(\theta_r) + q \cos(\theta_r)] \right] \tag{122}$$

$$\underline{H}_m^+ = \frac{k_m}{\omega\mu} \left[\hat{r} \cos(\theta_r) + \hat{q} \sin(\theta_r) \right] \, E_{mx}^+ \tag{123}$$

$$= \hat{r} \, H_{mr}^+ + \hat{q} \, H_{mq}^+ \tag{124}$$

where the superscript " + " indicates the wave traveling in the positive z direction within the material sample. The boundary conditions require that the tangential field components be continuous for all values of r along $q = 0$.

$$\hat{x} \cdot \underline{E}_i \, (q = 0-) = \hat{x} \cdot \underline{E}_m \, (q = 0+) \tag{125}$$

67

$$\exp[j \, k_o \, r \, \sin(\theta_i)] = \exp[j \, k_m \, r \, \sin(\theta_r)] \qquad (126)$$

$$k_o \, \sin(\theta_i) = k_m \, \sin(\theta_r) \qquad (127)$$

$$\frac{\sin(\theta_i)}{\sin(\theta_r)} = \frac{k_m}{k_o} \qquad (128)$$

$$= (\mu_r \epsilon_r)^{\frac{1}{2}} \qquad (129)$$

Denote the wave impedance of the sample in the direction of increasing q by Z_m. Then

$$Z_m = \frac{E_{mx}^+}{H_{mr}^+} \qquad (130)$$

$$= \frac{E_{mx}^+}{\dfrac{k_m}{\omega \mu} \, E_{mx}^+ \, \cos(\theta_r)} \qquad (131)$$

$$= \frac{\omega \mu}{\omega \, (\mu \epsilon)^{\frac{1}{2}} \, \cos(\theta_r)} \qquad (132)$$

$$Z_m = (\tfrac{\mu}{\epsilon})^{\frac{1}{2}} \, \sec(\theta_r) \qquad (133)$$

From Eq (129)

$$\sin^2(\theta_i) = \mu_r \, \epsilon_r \, \sin^2(\theta_r) \qquad (134)$$

$$= \mu_r \, \epsilon_r \, [1 - \cos^2(\theta_r)] \qquad (135)$$

68

$$\cos(\theta_r) = \left[\frac{\mu_r \epsilon_r - \sin^2\theta_i}{\mu_r \epsilon_r} \right]^{\frac{1}{2}} \tag{136}$$

$$Z_m = \frac{(\frac{\mu}{\epsilon})^{\frac{1}{2}} (\mu_r \epsilon_r)^{\frac{1}{2}}}{[\mu_r \epsilon_r - \sin^2(\theta_i)]^{\frac{1}{2}}} \tag{137}$$

$$= \frac{\mu_r (\frac{\mu_o}{\epsilon_o})^{\frac{1}{2}}}{[\mu_r \epsilon_r - \sin^2(\theta_i)]^{\frac{1}{2}}} \tag{138}$$

Normalizing $\quad Z = Z_m/Z_o$

$$Z = \frac{\mu_r (\frac{\mu_o}{\epsilon_o})^{\frac{1}{2}}}{[\mu_r \epsilon_r - \sin^2(\theta_i)]^{\frac{1}{2}}} \quad \frac{\cos(\theta_i)}{(\frac{\mu_o}{\epsilon_o})^{\frac{1}{2}}} \tag{139}$$

$$Z = \frac{\mu_r \cos(\theta_i)}{[\mu_r \epsilon_r - \sin^2(\theta_i)]^{\frac{1}{2}}} \tag{140}$$

Parallel Polarization. Rather than proceed through a derivation
similar to that for perpendicular polarization, advantage is taken of
the duality of electromagnetic fields and the result for parallel polar-
ization is obtained by means of the following transformation:

$$\underline{E}' = (\frac{\mu}{\epsilon})^{\frac{1}{2}} \underline{H} \tag{141}$$

$$\underline{H}' = -(\frac{\epsilon}{\mu})^{\frac{1}{2}} \underline{E} \tag{142}$$

where the primed variables denote the parallel case (2:29).

69

$$Z'_o = - \frac{E'_{ir}}{H'_{ix}} \tag{143}$$

$$= \frac{(\frac{\mu_o}{\epsilon_o})^{\frac{1}{2}} H_{ir}}{(\frac{\epsilon_o}{\mu_o})^{\frac{1}{2}} E_{ix}} \tag{144}$$

$$= \frac{(\frac{\mu_o}{\epsilon_o})^{\frac{1}{2}} \left[(\frac{\epsilon_o}{\mu_o})^{\frac{1}{2}} \cos(\theta_i) E_{ix} \right]}{(\frac{\epsilon_o}{\mu_o})^{\frac{1}{2}} E_{ix}} \tag{145}$$

$$= (\frac{\mu_o}{\epsilon_o})^{\frac{1}{2}} \cos(\theta_i) \tag{146}$$

$$Z'_m = - \frac{E^{+'}_{mr}}{H^{+'}_{mx}} \tag{147}$$

$$= \frac{(\frac{\mu}{\epsilon})^{\frac{1}{2}} H^{+}_{mr}}{(\frac{\epsilon}{\mu})^{\frac{1}{2}} E^{+}_{mx}} \tag{148}$$

$$= \frac{(\frac{\mu}{\epsilon})^{\frac{1}{2}} \left[\frac{k_m}{\omega\mu} E^{+}_{mx} \cos(\theta_r) \right]}{(\frac{\epsilon}{\mu})^{\frac{1}{2}} E^{+}_{mx}} \tag{149}$$

70

$$= \frac{(\frac{\mu}{\epsilon})^{\frac{1}{2}} (\frac{\epsilon}{\mu})^{\frac{1}{2}} \cos(\theta_r)}{(\frac{\epsilon}{\mu})^{\frac{1}{2}}} \qquad (150)$$

$$= (\frac{\mu}{\epsilon})^{\frac{1}{2}} \cos(\theta_r) \qquad (151)$$

$$= \frac{(\frac{\mu}{\epsilon})^{\frac{1}{2}} [\mu_r \epsilon_r - \sin^2(\theta_i)]^{\frac{1}{2}}}{(\mu_r \epsilon_r)^{\frac{1}{2}}} \qquad (152)$$

$$= (\frac{\mu}{\epsilon \mu_r \epsilon_r})^{\frac{1}{2}} [\mu_r \epsilon_r - \sin^2(\theta_i)]^{\frac{1}{2}} \qquad (153)$$

$$Z'_m = (\frac{\mu_o}{\epsilon_o})^{\frac{1}{2}} \frac{[\mu_r \epsilon_r - \sin^2(\theta_i)]^{\frac{1}{2}}}{\epsilon_r} \qquad (154)$$

$$Z' = \frac{Z'_m}{Z'_o} \qquad (155)$$

$$= \frac{(\frac{\mu_o}{\epsilon_o})^{\frac{1}{2}} [\mu_r \epsilon_r - \sin^2(\theta_i)]^{\frac{1}{2}}}{\epsilon_r \; (\frac{\mu_o}{\epsilon_o})^{\frac{1}{2}} \cos(\theta_i)} \qquad (156)$$

71

$$Z' = \frac{[\mu_r \epsilon_r - \sin^2(\theta_i)]^{\frac{1}{2}}}{\epsilon_r \cos(\theta_i)} \qquad (157)$$

Electrical Thickness

$$\delta = 2\pi \tau \qquad (158)$$

where τ is the number of wavelengths inside the sheet along the q direction.

$$\tau = \frac{d}{\lambda_q} \qquad (159)$$

$$\delta = 2\pi \left(\frac{d}{\lambda_q}\right) \qquad (160)$$

where λ_q is the wavelength inside the sheet along the q direction and d is the depth of the material.

$$\lambda_q = \frac{2\pi}{k_q} \qquad (161)$$

where k_q is the wavenumber corresponding to λ_q. The propagation factor of the wave inside the sheet along the q direction is

$$\exp\left[- j k_m[- r \sin(\theta_r) + q \cos(\theta_r)]\right] =$$

$$\exp(- j k_r r) \exp(- j k_q q) \qquad (162)$$

72

Therefore

$$k_q = k_m \cos(\theta_r) \qquad (163)$$

$$= \frac{k_o \, (\mu_r \epsilon_r)^{\frac{1}{2}} \, [\mu_r \epsilon_r - \sin^2(\theta_i)]^{\frac{1}{2}}}{(\mu_r \epsilon_r)^{\frac{1}{2}}} \qquad (164)$$

$$= k_o \, [u_r \epsilon_r - \sin^2(\theta_i)]^{\frac{1}{2}} \qquad (165)$$

$$= \left(\frac{2\pi}{\lambda_o}\right) [u_r \epsilon_r - \sin^2(\theta_i)]^{\frac{1}{2}} \qquad (166)$$

$$\delta = k_q \, d \qquad (167)$$

$$\delta = \left(\frac{2\pi \, d}{\lambda_o}\right) [u_r \epsilon_r - \sin^2(\theta_i)]^{\frac{1}{2}} \qquad (168)$$

where λ_0 is the free space wavelength.

Appendix B: Derivation of T^2 and the Gradient of G

Derivation of T^2

$$T = \frac{4\ Z}{(Z+1)^2\ e^{j\delta} - (Z-1)^2\ e^{-j\delta}} \tag{78}$$

$$= \frac{4\ Z\ e^{-j\delta}}{(Z+1)^2 - (Z-1)^2\ e^{-j2\delta}} \tag{169}$$

The superscript " $*$ " is used to denote the complex conjugate of a quantity.

$$T^2 = T\ T^* \tag{170}$$

where

$$T^* = \frac{4\ Z^*\ e^{j\delta*}}{(Z^*+1)^2 - (Z^*-1)^2\ e^{j2\delta*}} \tag{171}$$

$$T^2 = \frac{(4\ Z\ e^{-j\delta})\ (4\ Z^*\ e^{j\delta*})}{\left[(Z+1)^2 - (Z-1)^2\ e^{-j2\delta}\right]\left[(Z^*+1)^2 - (Z^*-1)^2\ e^{j2\delta*}\right]} \tag{172}$$

$$T^2 = 16\ Z\ Z^*\ e^{j(\delta*-\delta)}\ /\ \left[(Z+1)^2(Z^*+1)^2 + (Z-1)^2(Z^*-1)^2\right.$$

$$\left. e^{j2(\delta*-\delta)} - (Z+1)^2(Z^*-1)^2\ e^{j2\delta*} - (Z^*+1)^2(Z-1)^2\ e^{-j2\delta}\right] \tag{173}$$

Since Z and   are complex, they can be written in the form

$$Z = a + j b \tag{174}$$

$$\delta = s + j t \tag{175}$$

T^2 is derived in terms of a, b, s, and t and then the expressions for a, b, s, and t are derived in terms of ϵ and μ.

$\underline{\delta * - \delta.}$ $\delta * - \delta = (s - jt) - (s + jt) \tag{176}$

$$= - j2t \tag{177}$$

$\underline{Z \; Z^*.}$ $Z \; Z^* = (a + jb)(a - jb) \tag{178}$

$$= a^2 + b^2 \tag{179}$$

$\underline{(Z+1)^2 (Z^*+1)^2.}$

$$(Z+1)^2 (Z^*+1)^2 = \left[(Z+1)(Z^*+1) \right]^2 \tag{180}$$

$$= \left[Z \; Z^* + (Z+Z^*) + 1 \right]^2 \tag{181}$$

75

$$Z + Z^* = (a+jb) + (a-jb) \tag{182}$$

$$= 2a \tag{183}$$

$$(Z+1)^2(Z^*+1)^2 = (a^2+b^2+2a+1)^2 \tag{184}$$

$$= a^4+b^4+2a^2b^2+4a(a^2+b^2+1) + 6a^2+2b^2+1 \tag{185}$$

$$\underline{(Z-1)^2(Z^*-1)^2 \, e^{j2(\delta^*-\delta)}.}$$

$$(Z-1)^2(Z^*-1)^2 \, e^{j2(\delta^*-\delta)} = \left[(Z-1)(Z^*-1)\right]^2 \, e^{j2(\delta^*-\delta)} \tag{186}$$

$$= \left[Z \, Z^* - (Z+Z^*) + 1\right]^2 \, e^{j2(-j2t)} \tag{187}$$

$$= (a^2+b^2-2a+1)^2 \, e^{4t} \tag{188}$$

$$= (a^4+b^4+2a^2b^2-4a(a^2+b^2+1)+6a^2+2b^2+1)e^{4t} \tag{189}$$

$$\underline{(Z+1)^2(Z^*-1)^2.}$$

$$(Z+1)^2(Z^*-1)^2 = \left[(Z+1)(Z^*-1)\right]^2 \tag{190}$$

$$= \left[Z \, Z^* - (Z-Z^*)-1\right]^2 \tag{191}$$

76

$$Z - Z^* = (a+jb) - (a-jb) \qquad (192)$$

$$= j\,2\,b \qquad (193)$$

$$(Z+1)^2(Z^*-1)^2 = (a^2+b^2-1-j2b)^2 \qquad (194)$$

$$= (a^2+b^2-1)^2 - 4b^2 - j4b(a^2+b^2-1) \qquad (195)$$

$$= (a^4+b^4+2a^2b^2-2a^2-2b^2+1) - 4b^2 - j4b(a^2+b^2-1) \qquad (196)$$

$$= a^4+b^4+2a^2b^2-2a^2-6b^2+1-j4b(a^2+b^2-1) \qquad (197)$$

$$\underline{(Z^*+1)^2(Z-1)^2.}$$

$$(Z^*+1)^2(Z-1)^2 = \left[(Z+1)^2(Z^*-1)^2\right]^* \qquad (198)$$

$$= a^4+b^4+2a^2b^2-2a^2-6b^2+1+j4b(a^2+b^2-1) \qquad (199)$$

Let
$$(Z^*+1)^2 (Z-1)^2 = m+jn \qquad (200)$$

Then
$$(Z+1)^2 (Z^*-1)^2 = m-jn \qquad (201)$$

77

$$(Z+1)^2(Z^*-1)^2 e^{j2\delta^*} + (Z^*+1)^2(Z-1)^2 e^{-j2\delta}$$

$$= (m-jn) e^{j2\delta^*} + (m+jn) e^{-j2\delta} \qquad (202)$$

$$= (m-jn) e^{j2(s-jt)} + (m+jn) e^{-j2(s+jt)} \qquad (203)$$

$$= e^{2t} [m(e^{j2s}+e^{-j2s}) + jn(e^{-j2s}-e^{j2s})] \qquad (204)$$

$$= e^{2t} \left[2m \left(\frac{e^{j2s} + e^{-j2s}}{2}\right) + 2n \left(\frac{e^{j2s} - e^{-j2s}}{2j}\right)\right] \qquad (205)$$

$$= 2e^{2t} [m \cos(2s) + n \sin(2s)] \qquad (206)$$

The denominator (Den) of Eq (173) can be written

$$Den = (a^4+b^4+2a^2b^2+4a(a^2+b^2+1)+6a^2+2b^2+1)$$

$$+ e^{4t}(a^4+b^4+2a^2b^2-4a(a^2+b^2+1)+6a^2+2b^2+1)$$

$$- 2e^{2t} [m \cos(2s) + n \sin(2s)] \qquad (207)$$

78

Substituting for m and n and regrouping terms,

$$Den = (1+e^{4t})(a^4+b^4+2a^2b^2+6a^2+2b^2+1)+(1-e^{4t})(4a)(a^2+b^2+1)$$

$$- 2e^{2t}[a^4+b^4+2a^2b^2-2a^2-6b^2+1)\cos(2s)$$

$$+ 4b(a^2+b^2-1)\sin(2s)] \qquad (208)$$

$$T^2 = \frac{16(a^2+b^2)e^{2t}}{Den} \qquad (209)$$

Derivation of a and b.

Perpendicular Polarization.

$$Z = \frac{\mu\cos\theta}{[\mu\epsilon - \sin^2\theta]^{\frac{1}{2}}} \qquad (140)$$

where the subscripts "r" and "i" have been deleted for simplicity.

$$Z = \frac{(\mu'-j\mu'')\cos\theta}{[(\mu'-j\mu'')(\epsilon'-j\epsilon'') - \sin^2\theta]^{\frac{1}{2}}} \qquad (210)$$

$$= \frac{(\mu'-j\mu'')\cos\theta}{[(\mu'\epsilon'-\mu''\epsilon'' - \sin^2\theta) - j(\epsilon'\mu''+\epsilon''\mu')]^{\frac{1}{2}}} \qquad (211)$$

79

Let

$$\alpha = \mu'\epsilon' - \mu''\epsilon'' - \sin^2\theta \qquad (212)$$

$$\beta = \epsilon'\mu'' + \epsilon''\mu' \qquad (213)$$

$$[\alpha - j\beta]^{\frac{1}{2}} = f - jg \qquad (214)$$

Then

$$Z = \cos\theta \, \frac{\mu' - j\mu''}{f - jg} \qquad (215)$$

$$= \frac{\cos\theta}{f^2 + g^2} \left[(\mu'f + \mu''g) + j(\mu'g - \mu''f) \right] \qquad (216)$$

$$[\alpha - j\beta]^{\frac{1}{2}} = \left[\frac{\alpha + (\alpha^2 + \beta^2)^{\frac{1}{2}}}{2} \right]^{\frac{1}{2}} - j\left[\frac{-\alpha + (\alpha^2 + \beta^2)^{\frac{1}{2}}}{2} \right]^{\frac{1}{2}} \qquad (217)$$

Let

$$c_1 = [\alpha + (\alpha^2 + \beta^2)^{\frac{1}{2}}]^{\frac{1}{2}}$$

$$c_2 = [-\alpha + (\alpha^2 + \beta^2)^{\frac{1}{2}}]^{\frac{1}{2}}$$

$$f = \frac{c_1}{\sqrt{2}} \qquad (218)$$

$$g = \frac{c_2}{\sqrt{2}} \qquad (219)$$

80

$$f^2 + g^2 = \tfrac{1}{2}[\alpha + (\alpha^2 + \beta^2)^{\frac{1}{2}} - \alpha + (\alpha^2 + \beta^2)^{\frac{1}{2}}] \qquad (220)$$

$$= (\alpha^2 + \beta^2)^{\frac{1}{2}} \qquad (221)$$

Let

$$c_3 = (\alpha^2 + \beta^2)^{\frac{1}{2}}$$

$$Z = \frac{\cos\theta}{c_3}\left[(\mu' f + \mu'' g) + j(\mu' g - \mu'' f)\right] \qquad (222)$$

Therefore

$$a = \frac{\cos\theta}{\sqrt{2}\ c_3}\left[c_1\mu' + c_2\mu''\right] \qquad (223)$$

$$b = \frac{\cos\theta}{\sqrt{2}\ c_3}\left[c_2\mu' - c_1\mu''\right] \qquad (224)$$

Parallel Polarization. From Eq (157)

$$Z = \frac{\left[\mu\,\epsilon - \sin^2\theta\right]^{\frac{1}{2}}}{\epsilon\cos\theta} \qquad (225)$$

$$= \frac{1}{\cos\theta}\ \frac{f - jg}{\epsilon' - j\epsilon''} \qquad (226)$$

81

$$Z = \frac{1}{[(\epsilon')^2 + (\epsilon'')^2]\cos\theta} \left[(\epsilon'f + \epsilon''g) + j(\epsilon''f - \epsilon'g)\right] \quad (227)$$

Let

$$c_4 = (\epsilon')^2 + (\epsilon'')^2$$

Therefore

$$a = \frac{1}{\sqrt{2} \, c_4 \cos\theta} \left[c_1 \epsilon' + c_2 \epsilon''\right] \quad (228)$$

$$b = \frac{1}{\sqrt{2} \, c_4 \cos\theta} \left[c_1 \epsilon'' - c_2 \epsilon'\right] \quad (229)$$

Derivation of s and t.   From Eqs (168) and (214)

$$\delta = \left(\frac{2\pi d}{\lambda_o}\right) \left[\mu \, \epsilon - \sin^2\theta\right]^{\frac{1}{2}} \quad (168)$$

$$= \left(\frac{2\pi d}{\lambda_o}\right) (f - jg) \quad (230)$$

Therefore

$$s = \sqrt{2} \, \pi \left(\frac{d}{\lambda_o}\right) c_1 \quad (231)$$

$$t = -\sqrt{2} \, \pi \left(\frac{d}{\lambda_o}\right) c_2 \quad (232)$$

82

Derivation of the Gradient of G

From Eq (100)

$$G(\epsilon', \epsilon'', \mu', \mu'') = \sum_{n=1}^{4} \left[F_n(\epsilon', \epsilon'', \mu', \mu'') \right]^2 \qquad (233)$$

To enable the use of vector notation, denote the set of four unknown material parameters ϵ', ϵ'', μ', and μ'' by the vector $\underline{x} = [x_1, x_2, x_3, x_4]$. The gradient of $G(\underline{x})$, grad $G(\underline{x})$, is given by

$$\text{grad } G(\underline{x}) = \left[\frac{\partial}{\partial x_1} G(\underline{x}), \frac{\partial}{\partial x_2} G(\underline{x}), \frac{\partial}{\partial x_3} G(\underline{x}), \frac{\partial}{\partial x_4} G(\underline{x}) \right] \qquad (234)$$

Denote any one of the x_n by x. Then

$$\frac{\partial}{\partial x} G(\underline{x}) = \frac{\partial}{\partial x} \left[\sum_{n=1}^{4} F_n^2 \right] \qquad (235)$$

$$= \sum_{n=1}^{4} \frac{\partial}{\partial x} \left[F_n^2 \right] \qquad (236)$$

$$= 2 \sum_{n=1}^{4} \frac{\partial}{\partial x} \left[F_n \right] \qquad (237)$$

$$= 2 \sum_{n=1}^{4} \frac{\partial}{\partial x} \left[T_n^2 - A_n \right] \qquad (238)$$

$$= 2 \sum_{n=1}^{4} \frac{\partial}{\partial x} \left[T_n^2 \right] \qquad (239)$$

83

Thus the derivative of T^2 with respect to each of the four material parameters must be obtained. The development will be presented in terms of a generic material parameter " x " as far as possible and then substitutions for the actual parameters will be given.

$$\frac{\partial}{\partial x} T^2.$$

$$T^2 = \frac{16 (a^2+b^2) e^{2t}}{A + 4B - 2C - 8D} \tag{240}$$

Let

$$c_5 = a^4 + b^4 + 2a^2b^2 + 6a^2 + 2b^2 + 1$$

$$c_6 = (a^2 + b^2 + 1)$$

$$c_7 = a^4 + b^4 + 2a^2b^2 - 2a^2 - 6b^2 + 1$$

$$c_8 = (a^2 + b^2 - 1)$$

Then

$$A = c_5 (1 + e^{4t}) \tag{241}$$

$$B = c_6 a(1 - e^{4t}) \tag{242}$$

$$C = c_7 e^{2t} \cos(2s) \tag{243}$$

$$D = c_8 b e^{2t} \sin(2s) \tag{244}$$

84

and a and b are given by Eqs (223), (224), and (228), (229) for perpen-
dicular and parallel polarization respectively. Let "Num" and "Den"
stand for the numerator and denominator of Eq (240). Then

$$\frac{\partial}{\partial x}\left[T^2\right] = \frac{Den \frac{\partial}{\partial x}(Num) - Num \frac{\partial}{\partial x}(Den)}{(Den)^2}. \qquad (245)$$

where

$$\frac{\partial}{\partial x}(Num) = 32e^{2t}\left[a\frac{\partial}{\partial x}(a) + b\frac{\partial}{\partial x}(b) + (a^2+b^2)\frac{\partial}{\partial x}(t)\right] \qquad (246)$$

$$\frac{\partial}{\partial x}(Den) = \frac{\partial}{\partial x}(A) + 4\frac{\partial}{\partial x}(B) - 2\frac{\partial}{\partial x}(C) - 8\frac{\partial}{\partial x}(D) \qquad (247)$$

$$\frac{\partial}{\partial x}(A) = 4\left[c_5\,e^{4t}\,\frac{\partial}{\partial x}(t) \right.$$
$$\left. + (1+e^{4t})\left[a(a^2+b^2+3)\frac{\partial}{\partial x}(a) + c_6\,b\frac{\partial}{\partial x}(b)\right]\right] \qquad (248)$$

$$\frac{\partial}{\partial x}(B) = -4\,c_6\,ae^{4t}\,\frac{\partial}{\partial x}(t) + (1-e^{4t})\left[(3a^2+b^2+1)\frac{\partial}{\partial x}(a) + 2ab\frac{\partial}{\partial x}(b)\right]$$
$$(249)$$

$$\frac{\partial}{\partial x}(C) = 2e^{2t}\left[c_7\left[\cos(2s)\,\frac{\partial}{\partial x}(t) - \sin(2s)\,\frac{\partial}{\partial x}(t)\right]\right.$$
$$\left. + 2\cos(2s)\left[c_8\,a\,\frac{\partial}{\partial x}(a)+b(a^2+b^2-3)\frac{\partial}{\partial x}(b)\right]\right] \qquad (250)$$

85

$$\frac{\partial}{\partial x}(D) = e^{2t}\left[2c_8 b\left[\sin(2s)\frac{\partial}{\partial x}(t) + \cos(2s)\frac{\partial}{\partial x}(s)\right]\right.$$

$$\left. + \sin(2s)\left[2ab\frac{\partial}{\partial x}(a) + (a^2 + 3b^2 - 1)\frac{\partial}{\partial x}(b)\right]\right] \qquad (251)$$

The expressions for $\frac{\partial}{\partial x}(s)$, $\frac{\partial}{\partial x}(t)$, $\frac{\partial}{\partial x}(a)$, and $\frac{\partial}{\partial x}(b)$ are derived for each x (that is, ϵ', ϵ'', μ', and μ'') and then substituted into the above equations to arrive at grad $G(\underline{x})$. The expressions for s and t are the same under either polarization but those for a and b must be derived for each polarization separately.

To simplify the following expressions let

$$c_9 = \frac{\pi\ d}{\sqrt{2}\ \lambda_o}$$

$$k_1 = \alpha\mu' + \beta\mu''$$

$$k_2 = \beta\mu' - \alpha\mu''$$

$$k_3 = \alpha\epsilon' + \beta\epsilon''$$

$$k_4 = \beta\epsilon' - \alpha\epsilon''$$

Perpendicular Polarization

$$\underline{\frac{\partial}{\partial x}\ (s).}$$

$$\frac{\partial}{\partial\epsilon'}(s) = \left(\frac{c_9}{c_1}\right)\left[\mu' + \left(\frac{k_1}{c_3}\right)\right] \qquad (252)$$

$$\frac{\partial}{\partial\epsilon''}(s) = \left(\frac{c_9}{c_1}\right)\left[-\mu'' + \left(\frac{k_2}{c_3}\right)\right] \qquad (253)$$

86

$$\frac{\partial}{\partial \mu'}(s) = \left(\frac{c_9}{c_1} \right)\left[\epsilon' + \left(\frac{k_3}{c_3}\right)\right] \qquad (254)$$

$$\frac{\partial}{\partial \mu''}(s) = \left(\frac{c_9}{c_1} \right)\left[-\epsilon'' + \left(\frac{k_4}{c_3}\right)\right] \qquad (255)$$

$$\underline{\frac{\partial}{\partial x}(t).}$$

$$\frac{\partial}{\partial \epsilon'}(t) = \left(-\frac{c_9}{c_2}\right)\left[-\mu' + \left(\frac{k_1}{c_3}\right)\right] \qquad (256)$$

$$\frac{\partial}{\partial \epsilon''}(t) = \left(-\frac{c_9}{c_2}\right)\left[\mu'' + \left(\frac{k_2}{c_3}\right)\right] \qquad (257)$$

$$\frac{\partial}{\partial \mu'}(t) = \left(-\frac{c_9}{c_2}\right)\left[-\epsilon' + \left(\frac{k_3}{c_4}\right)\right] \qquad (258)$$

$$\frac{\partial}{\partial \mu''}(t) = \left(-\frac{c_9}{c_2}\right)\left[\epsilon'' + \left(\frac{k_4}{c_4}\right)\right] \qquad (259)$$

87

$$\frac{\partial}{\partial x}(a) \ .$$

$$\frac{\partial}{\partial \epsilon'}(a) = \frac{\cos \theta}{\sqrt{2}\ c_3} \left[\frac{\mu'}{2c_1}[\mu'+(\frac{k_1}{c_3})]+\frac{\mu''}{2c_2}[-\mu'+(\frac{k_1}{c_3})] \right.$$

$$\left. - (\frac{k_1}{c_3^2})(c_1\mu' + c_2\mu'') \right] \qquad (260)$$

$$\frac{\partial}{\partial \epsilon''}(a) = \frac{\cos \theta}{\sqrt{2}\ c_3} \left[\frac{\mu'}{2c_1}[-\mu''+(\frac{k_2}{c_3})]+\frac{\mu''}{2c_2}[\mu''+(\frac{k_2}{c_3})] \right.$$

$$\left. - (\frac{k_2}{c_3^2})(c_1\mu' + c_2\mu'') \right] \qquad (261)$$

$$\frac{\partial}{\partial \mu'}(a) = \frac{\cos \theta}{\sqrt{2}\ c_3} \left[c_1 + \frac{\mu'}{2c_1}[\epsilon'+(\frac{k_3}{c_3})]+\frac{\mu''}{2c_2}[-\epsilon'+(\frac{k_3}{c_3})] \right.$$

$$\left. - (\frac{k_3}{c_3^2})(c_1\mu'+c_2\mu'') \right] \qquad (262)$$

$$\frac{\partial}{\partial \mu''}(a) = \frac{\cos \theta}{\sqrt{2}\ c_3} \left[\frac{\mu'}{2c_1}[-\epsilon''+(\frac{k_4}{c_3})]+c_2+\frac{\mu''}{2c_2}[\epsilon''+(\frac{k_4}{c_3})] \right.$$

$$\left. - (\frac{k_4}{c_3^2})(c_1\mu'+c_2\mu'') \right] \qquad (263)$$

88

$$\frac{\partial}{\partial x}(b) \ .$$

$$\frac{\partial}{\partial \epsilon'}(b) = \frac{\cos \theta}{\sqrt{2} \ c_3} \left[\frac{\mu'}{2c_2}\left[-\mu'+(\frac{k_1}{c_3})\right] - \frac{\mu''}{2c_1}\left[\mu'+(\frac{k_1}{c_3})\right] \right.$$

$$\left. - (\frac{k_1}{c_3^2})(c_2\mu' - c_1\mu'') \right] \tag{264}$$

$$\frac{\partial}{\partial \epsilon''}(b) = \frac{\cos \theta}{\sqrt{2} \ c_3} \left[\frac{\mu'}{2c_2}\left[\mu''+(\frac{k_2}{c_3})\right] - \frac{\mu''}{2c_1}\left[-\mu''+(\frac{k_2}{c_3})\right] \right.$$

$$\left. - (\frac{k_2}{c_3^2})(c_2\mu' - c_1\mu'') \right] \tag{265}$$

$$\frac{\partial}{\partial \mu'}(b) = \frac{\cos \theta}{\sqrt{2} \ c_3} \left[c_2 + \frac{\mu'}{2c_2}\left[-\epsilon'+(\frac{k_3}{c_3})\right] - \frac{\mu''}{2c_1}\left[\epsilon'+(\frac{k_3}{c_3})\right] \right.$$

$$\left. - (\frac{k_3}{c_3^2})(c_2\mu' - c_1\mu'') \right] \tag{266}$$

$$\frac{\partial}{\partial \mu''}(b) = \frac{\cos\theta}{\sqrt{2}\; c_3}\left[\frac{\mu'}{2c_2}\left[\epsilon''+(\frac{k_4}{c_3})\right]-c_1-\frac{\mu''}{2c_1}\left[-\epsilon''+(\frac{k_4}{c_3})\right]\right.$$

$$\left.- (\frac{k_4}{c_3{}^2})(c_2\mu' - c_1\mu'')\right] \tag{267}$$

Parallel Polarization

$$\frac{\partial}{\partial x}\ (a)\ .$$

$$\frac{\partial}{\partial \epsilon'}(a) = (\sqrt{2}\; c_4 \cos\theta)^{-1}\left[c_1+\frac{\epsilon'}{2c_1}\left[\mu'+(\frac{k_1}{c_3})\right]+\frac{\epsilon''}{2c_2}\left[-\mu'+(\frac{k_1}{c_3})\right]\right.$$

$$\left.- (\frac{2\epsilon'}{c_4})(c_1\epsilon' + c_2\epsilon'')\right] \tag{268}$$

$$\frac{\partial}{\partial \epsilon''}(a) = (\sqrt{2}\; c_4 \cos\theta)^{-1}\left[\frac{\epsilon'}{2c_1}\left[-\mu''+(\frac{k_2}{c_3})\right]+c_2+\frac{\epsilon''}{2c_2}\left[\mu''+(\frac{k_2}{c_3})\right]\right.$$

$$\left.- (\frac{2\epsilon''}{c_4})(c_1\epsilon' + c_2\epsilon'')\right] \tag{269}$$

$$\frac{\partial}{\partial \mu'}(a) = (\sqrt{2}\; c_4 \cos\theta)^{-1}\left[\frac{\epsilon'}{2c_1}\left[\epsilon'+(\frac{k_3}{c_3})\right]+\frac{\epsilon''}{2c_2}\left[-\epsilon'+(\frac{k_3}{c_3})\right]\right] \tag{270}$$

90

$$\frac{\partial}{\partial \mu''}(a) = (\sqrt{2}\, c_4 \cos\theta)^{-1}\left[\frac{\epsilon'}{2c_1}\left[-\epsilon''+(\frac{k_4}{c_3})\right]+\frac{\epsilon''}{2c_2}\left[\epsilon''+(\frac{k_4}{c_3})\right]\right] \quad (271)$$

$$\frac{\partial}{\partial x}(b) \; .$$

$$\frac{\partial}{\partial \epsilon'}(b) = (\sqrt{2}\, c_4 \cos\theta)^{-1}\left[-c_2-\frac{\epsilon'}{2c_2}\left[-\mu'+(\frac{k_1}{c_3})\right]+\frac{\epsilon''}{2c_1}\left[\mu'+(\frac{k_1}{c_3})\right]\right.$$
$$\left. -(\frac{2\epsilon'}{c_4})(c_1\epsilon''-c_2\epsilon')\right] \quad (272)$$

$$\frac{\partial}{\partial \epsilon''}(b) = (\sqrt{2}\, c_4 \cos\theta)^{-1}\left[-\frac{\epsilon'}{2c_2}\left[\mu''+(\frac{k_2}{c_3})\right]+c_1+\frac{\epsilon''}{2c_1}\left[-\mu''+(\frac{k_2}{c_3})\right]\right.$$
$$\left. -(\frac{2\epsilon''}{c_4})(c_2\epsilon''-c_2\epsilon')\right] \quad (273)$$

$$\frac{\partial}{\partial \mu'}(b) = (\sqrt{2}\, c_4 \cos\theta)^{-1}\left[-\frac{\epsilon'}{2c_2}\left[-\epsilon'+(\frac{k_3}{c_3})\right]+\frac{\epsilon''}{2c_1}\left[\epsilon'+(\frac{k_3}{c_3})\right]\right] \quad (274)$$

$$\frac{\partial}{\partial \mu''}(b) = (\sqrt{2}\, c_4 \cos\theta)^{-1}\left[-\frac{\epsilon'}{2c_2}\left[\epsilon''+(\frac{k_4}{c_3})\right]+\frac{\epsilon''}{2c_1}\left[-\epsilon''+(\frac{k_4}{c_3})\right]\right] \quad (275)$$

The expressions for the nonmagnetic case are not shown explicitly. They can be obtained from the general expressions by substituting $\mu' = 1$, $\mu'' = 0$, and deleting the derivatives with respect to μ' and μ''.

91

Bibliography

1. Kent, Brian. *An Automated Dual Horn-Reflector Microwave Absorber Measurement System.* Technical Report AFWAL-TR-81-1284. Avionics Laboratory (AFWAL/AAWP-3), Air Force Wright Aeronautical Laboratories (AFSC), Wright-Patterson AFB OH, June 1982.

2. Collin, Robert E. *Field Theory of Guided Waves.* New York: McGraw-Hill Book Company, 1960.

3. Kouyoumjian, R. G. and L. Peters, Jr. "Range Requirements in Radar Cross-Section Measurements," *Proceedings of the IEEE, 53:* 920-928 (August 1965).

4. Mentzer, J. R. "The Use of Dielectric Lenses in Reflection Measurements," *Proceedings of the I.R.E., 41:* 252-256 (February 1953).

5. Redheffer, R. M. "The Measurement of Dielectric Constants," *Techniques of Microwave Measurements, Volume 11,* edited by Carol G. Montgomery. New York: McGraw-Hill Book Company, 1947.

6. von Hippel, Arthur R. *Dielectrics and Waves.* New York: John Wiley & Sons, and The Technology Press of M.I.T., 1954.

7. Collin, Robert E. *Foundations for Microwave Engineering.* New York: McGraw-Hill Book Company, 1966.

8. Jones, Douglas S. *The Theory of Electromagnetism.* Pergamon Press, 1964.

9. Kraus, John D. *Electromagnetics* (Third Edition). New York: McGraw Hill Book Company, 1984.

10. Burden, Richard L. and J. Douglas Faires. *Numerical Analysis* (Third Edition). Boston: Prindle, Weber and Schmidt, 1985.

11. Forsythe, George E. and others. *Computer Methods for Mathematical Computations.* Englewood Cliffs: Prentice-Hall, 1977.

12. von Hippel, Arthur R., ed. *Dielectric Materials and Applications.* New York: John Wiley & Sons, and The Technology Press of M.I.T., 1954.

13. Kent, Brian and Chizever, Hirsch. _An Automated Frequency Domain Microwave Absorber Measurement System For K-Band (18-26 GHz)._ Technical Report AFWAL-TM-83-23. Avionics Laboratory (AFWA. AAWP-3), Air Force Wright Aeronautical Laboratories (AFSC), Wright-Patterson AFB OH, July 1983.

Lieutenant John C. Joseph ███████████████████

████████████████ He graduated from high school in Bellingham, Massachusetts, in 1978 and attended the New England Conservatory of Music until June 1981. He entered the University of Lowell, Lowell, Massachusetts in September 1981 and received the degree of Bachelor of Science in Electrical Engineering in December 1984. He was employed as an associate engineer in the production of microstrip and stripline circuits for M/A-COM Inc., Burlington, Massachusetts until January 1985. Upon graduation, he received a commission in the USAF through the ROTC program and entered the Air Force on active duty in January 1985. He served as a laboratory engineer at the School of Engineering, Air Force Institute of Technology, until beginning the master's degree program in July 1985.

████████████   ███████████

██████████████   ████

ADA 178 851

REPORT DOCUMENTATION PAGE	Form Approved OMB No. 0704-0188

1a. REPORT SECURITY CLASSIFICATION UNCLASSIFIED	1b. RESTRICTIVE MARKINGS

2a. SECURITY CLASSIFICATION AUTHORITY	3. DISTRIBUTION/AVAILABILITY OF REPORT
2b. DECLASSIFICATION/DOWNGRADING SCHEDULE	Approved for public release; distribution unlimited.

4. PERFORMING ORGANIZATION REPORT NUMBER(S) AFIT/GE/ENG/86D-58	5. MONITORING ORGANIZATION REPORT NUMBER(S)

6a. NAME OF PERFORMING ORGANIZATION School of Engineering	6b. OFFICE SYMBOL (If applicable) AFIT/ENC	7a. NAME OF MONITORING ORGANIZATION

6c. ADDRESS (City, State, and ZIP Code) Air Force Institute of Technology Wright-Patterson AFB, Ohio 45433-6583	7b. ADDRESS (City, State, and ZIP Code)

8a. NAME OF FUNDING/SPONSORING ORGANIZATION AFWAL AAWP-3	8b. OFFICE SYMBOL (If applicable)	9. PROCUREMENT INSTRUMENT IDENTIFICATION NUMBER

8c. ADDRESS (City, State, and ZIP Code) Wright-Patterson AFB Ohio 45433	10. SOURCE OF FUNDING NUMBERS			
	PROGRAM ELEMENT NO.	PROJECT NO.	TASK NO	WORK UNIT ACCESSION NO

11. TITLE (Include Security Classification)
MULTIPLE ANGLE OF INCIDENCE MEASUREMENT TECHNIQUE FOR THE PERMITTIVITY AND PERMEABILITY OF LOSSY MATERIALS AT MILLIMETER WAVELENGTHS

12. PERSONAL AUTHOR(S)
John C. Joseph, B.S.E.E., 2d Lt, USAF

13a. TYPE OF REPORT MS Thesis	13b. TIME COVERED FROM_____ TO_____	14. DATE OF REPORT (Year, Month, Day) 1986 December	15. PAGE COUNT 103

16. SUPPLEMENTARY NOTATION

17. COSATI CODES			18. SUBJECT TERMS (Continue on reverse if necessary and identify by block number)
FIELD	GROUP	SUB-GROUP	Radar Absorbing Materials, Electrical Measurement
14	02		Millimeter Waves
11			

19. ABSTRACT (Continue on reverse if necessary and identify by block number)

Thesis Chairman: Randy J. Jost, Captain, USAF

Approved for public release: IAW AFR 190-1.
LYNN E. WOLAVER 5 Mar 87
Dean for Research and Professional Development
Air Force Institute of Technology (ATC)
Wright-Patterson AFB OH 45433

20. DISTRIBUTION/AVAILABILITY OF ABSTRACT ☒ UNCLASSIFIED/UNLIMITED ☐ SAME AS RPT ☐ DTIC USERS	21. ABSTRACT SECURITY CLASSIFICATION UNCLASSIFIED
22a NAME OF RESPONSIBLE INDIVIDUAL Randy J. Jost, Captain, USAF	22b TELEPHONE (Include Area Code) 513-255-3576	22c OFFICE SYMBOL AFIT/ENG

DD Form 1473, JUN 86	Previous editions are obsolete.	SECURITY CLASSIFICATION OF THIS PAGE

A technique of measuring the permittivity and permeability of lossy, homogeneous, linear, isotropic materials at millimeter wavelengths was developed. The technique was tested by measurement of representative materials at a frequency of 94 GHz.

For the type of materials under consideration, the permittivity and permeability are complex in general. Thus there are four unknown. to be determined and a minimum of four measurements are required. The approach taken was to measure the magnitude of the transmission coefficient of a planar material sample in free space at multiple angles of incidence. The system of equations obtained from any four of the angles is solved numerically for the permittivity and permeability of the sample.

The equipment consisted primarily of a Gunn phase-locked millimeter-wave oscillator, a pair of conical horn/lens antennae, a sample holder/positioner, and a microwave receiver. Harmonic mixing was employed to convert the test waveform to the operating range of the receiver.

For the case of nonmagnetic materials, best results were obtained if the numerical solution was specialized to incorporate the assumption that the permeability of the material is equal to the permeability of free space. For a material of arbitrary permeability, it was necessary to take data at both perpendicular and parallel polarization of the incident wave to obtain satisfactory results.